BAW-1834

May 1984

ANALYSES OF CAPSULE TE1-B
THE TOLEDO EDISON COMPANY
DAVIS-BESSE NUCLEAR POWER STATION UNIT 1

-- Reactor Vessel Material Surveillance Program --

Babcock & Wilcox

a McDermott company

BAW-1834

May 1984

ANALYSES OF CAPSULE TE1-B
THE TOLEDO EDISON COMPANY
DAVIS-BESSE NUCLEAR POWER STATION UNIT 1

-- Reactor Vessel Material Surveillance Program --

by

A. L. Lowe, Jr., PE
L. L. Collins
J. W. Ewing
W. A. Pavinich
W. L. Redd

B&W Contract No. 582-7168

BABCOCK & WILCOX
Utility Power Generation Division
P. O. Box 1260
Lynchburg, Virginia 24505

Babcock & Wilcox
a McDermott company

SUMMARY

This report describes the results of the examination of the second capsule of the Toledo Edison Company's Davis-Besse Nuclear Power Station Unit 1 reactor vessel surveillance program. The capsule was removed and examined at the end of the third fuel cycle. The objective of the program is to monitor the effects of neutron irradiation on the tensile and fracture toughness properties of the reactor vessel materials by the testing and evaluation of tension, Charpy impact, and compact fracture toughness specimens. The program was designed in accordance with the requirements of Appendix H to 10 CFR 50 and ASTM specification E185-73.

The capsule received an average fast fluence of 5.92×10^{18} n/cm^2 (E > 1.0 MeV) and the predicted fast fluence for the reactor vessel T/4 location at the end of the third cycle is 8.4×10^{17} n/cm^2 (E > MeV). Based on the calculated fast flux at the vessel wall, an 80% load factor, and the planned fuel management, the projected fast fluence that the Davis-Besse Unit 1 reactor pressure vessel will receive in 40 calendar years' of operation is 1.6×10^{19} n/cm^2 (E > 1 MeV).

The results of the tension tests indicated that the materials exhibited normal behavior relative to neutron fluence exposure. The Charpy impact data results exhibited the characteristic behavior of shift to higher temperature for both the 30 and 50 ft-lb transition temperatures as a result of neutron fluence damage and a decrease in upper shelf energy. These results demonstrated that the current techniques used for predicting the change in both the increase in the RT_{NDT} and the decrease in upper shelf properties due to irradiation are conservative. The compact fracture toughness specimens were not tested at this time because no approved testing procedure was available. The results of these tests are the subject of a separate report.

The recommended operating period was extended to 15 effective full power years as a result of the second capsule evaluation. These new operating limitations are in accordance with the requirements of Appendix G of 10 CFR 50.

CONTENTS

CONTENTS (Cont'd)

List of Tables

Tables (Cont'd)

List of Figures

1. INTRODUCTION

This report describes the results of the examination of the second capsule of the Toledo Edison Company's Davis-Besse Nuclear Power Station Unit 1 reactor vessel material surveillance program. The capsule was removed and examined at the end of the third fuel cycle. The first capsule of the program was removed and examined after the first year of operation; the results are reported in BAW-1701.[1]

The objective of the program is to monitor the effects of neutron irradiation on the tensile and impact properties of reactor pressure vessel materials under actual operating conditions. The surveillance program for Davis-Besse Unit 1 was designed and furnished by Babcock & Wilcox (B&W) as described in BAW-10100A.[2] The program, designed in accordance with the requirements of Appendix H to 10 CFR 50* and ASTM Specification E185-73 and was planned to monitor the effects of neutron irradiation on the reactor vessel material for the 40-year design life of the reactor pressure vessel. The future operating limitations established after the evaluation of the surveillance capsule are also in accordance with the requirements of 10 CFR 50, Appendixes G and H. The recommended operating period was extended to 15 effective full power years (EFPY) as a result of the second capsule evaluation.

- - - - -

*Code of Federal Regulations, Title 10, Part 50.

2. BACKGROUND

The ability of the reactor pressure vessel to resist fracture is the primary factor in ensuring the safety of the primary system in light water-cooled reactors. The beltline region of the reactor vessel is the most critical region of the vessel because it is exposed to neutron irradiation. The general effects of fast neutron irradiation on the mechanical properties of such low-alloy ferritic steels as SA508, Class 2, used in the fabrication of the Davis-Besse Unit 1 reactor vessel, are well characterized and documented in the literature. The low-alloy ferritic steels used in the beltline region of reactor vessels exhibit an increase in ultimate and yield strength properties with a corresponding decrease in ductility after irradiation. The most serious mechanical property change in reactor pressure vessel steels is the increase in temperature for the transition from brittle to ductile fracture accompanied by a reduction in the Charpy upper shelf impact toughness.

Appendix G to 10 CFR 50, "Fracture Toughness Requirements," specifies minimum fracture toughness requirements for the ferritic materials of the pressure-retaining components of the reactor coolant pressure boundary (RCPB) of water-cooled power reactors, and provides specific guidelines for determining the pressure-temperature limitations on operation of the RCPB. The toughness and operational requirements are specified to provide adequate safety margins during any condition of normal operation, including anticipated operational occurrences and system hydrostatic tests, to which the pressure boundary may be subjected over its service lifetime. Although the requirements of Appendix G to 10 CFR 50 became effective on August 13, 1973, the requirements are applicable to all boiling and pressurized water-cooled nuclear power reactors, including those under construction or in operation on the effective date.

Appendix H to 10 CFR 50, "Reactor Vessel Materials Surveillance Program Requirements," defines the material surveillance program required to monitor changes in the fracture toughness properties of ferritic materials in the reactor vessel beltline region of water-cooled reactors resulting from exposure to neutron irradiation and the thermal environment. Fracture toughness test data are obtained from material specimens withdrawn periodically from the reactor vessel. These data will permit determination of the conditions under which the vessel can be operated with adequate safety margins against fracture throughout its service life.

A method for guarding against brittle fracture in reactor pressure vessels is described in Appendix G to the ASME Boiler and Pressure Vessel Code, Section III, "Nuclear Power Plant Components." This method utilizes fracture mechanics concepts and the reference nil-ductility temperature, RT_{NDT}, which is defined as the greater of the drop weight nil-ductility transition temperature (per ASTM E-208) or the temperature that is 60F below that at which the material exhibits 50 ft-lbs and 35 mils lateral expansion. The RT_{NDT} of a given material is used to index that material to a reference stress intensity factor curve (K_{IR} curve), which appears in Appendix G of ASME Section III. The K_{IR} curve is a lower bound of dynamic, static, and crack arrest fracture toughness results obtained from several heats of pressure vessel steel. When a given material is indexed to the K_{IR} curve, allowable stress intensity factors can be obtained for this material as a function of temperature. Allowable operating limits can then be determined using these allowable stress intensity factors.

The RT_{NDT} and, in turn, the operating limits of a nuclear power plant, can be adjusted to account for the effects of radiation on the properties of the reactor vessel materials. The radiation embrittlement and the resultant changes in mechanical properties of a given pressure vessel steel can be monitored by a surveillance program in which a surveillance capsule containing prepared specimens of the reactor vessel materials is periodically removed from the operating nuclear reactor and the specimens are tested. The increase in the Charpy V-notch 30 ft-lb temperature is added to the original RT_{NDT} to adjust it for radiation embrittlement. This adjusted RT_{NDT} is used to index the material to the K_{IR} curve which, in turn, is used to set operating limits for the nuclear power plant. These new limits take into account the effects of irradiation on the reactor vessel materials.

3. SURVEILLANCE PROGRAM DESCRIPTION

The surveillance program comprises six surveillance capsules designed to monitor the effects of neutron and thermal environment on the materials of the reactor pressure vessel core region. The capsules, which were inserted into the reactor vessel before initial plant startup, were positioned inside the reactor vessel between the thermal shield and the vessel wall at the locations shown in Figure 3-1. The six capsules, originally designed to be placed two in each holder tube, are positioned near the peak axial and azimuthal neutron flux. However, with the use of Davis-Besse Unit 1 as one of the irradiation sites of the 177 fuel assembly integrated reactor vessel material surveillance program, the capsules are irradiated on a schedule integrated with the capsules of the other participating reactors. This integrated schedule is described in BAW-1543.[3] BAW-10100A includes a full description of the capsule design.

Capsule TE1-B was removed during the third refueling shutdown of Davis- Besse Unit 1. This capsule contained Charpy V-notch impact and tension test specimens fabricated from base metal (SA508, Class 2) and weld metal, and weld metal compact fracture specimens. The specimens contained in the capsule are described in Table 3-1, and the location of the individual specimens within the capsule are described in Figure 3-2. The chemical composition and heat treatment of the surveillance material in capsule TE1-B are described in Table 3-2.

All test specimens were machined from the 1/4-thickness (1/4T) location of the forging material. Charpy V-notch and tension test specimens from the vessel material were oriented with their longitudinal axes perpendicular to the principal working direction of the forging. Capsule TE1-B contained dosimeter wires, described as follows:

Dosimeter wire	Shielding
U-Al alloy	Cd-Ag alloy
Np-Al alloy	Cd-Ag alloy
Nickel	Cd-Ag alloy
0.66 wt % Co-Al alloy	Cd-Ag alloy
0.66 wt % Co-Al alloy	None
Fe	None

Thermal monitors of low-melting eutectic alloys were included in the capsule. The eutectic alloys and their melting points are as follows:

Alloy	Melting point, F
90% Pb, 5% Ag, 5% Sn	558
97.5% Pb, 2.5% Ag	580
97.5% Pb, 1.5% Ag, 1.0% Sn	588
Cadmium	610
Lead	621

Table 3-1. Specimens in Surveillance Capsule TE1-B

	Number of test specimens		
Material description	Tension	CVN impact	1/2T compact fracture[a]
Weld metal	2	12	8
Weld-HAZ Heat SS, transverse	--	12	--
Base metal Heat SS, transverse	2	12	--
Total per capsule	4	36	8

[a]Compact fracture toughness specimens precracked per ASTM E399-72.

Table 3-2. Chemical Composition and Heat Treatment of Surveillance Materials

Chemical Analysis

Element	Heat[a] BCC241	Weld metal WF-182-1[b]
C	0.22	0.09
Mn	0.63	1.69
P	0.011	0.014
S	0.011	0.013
Si	0.27	0.41
Ni	0.81	0.63
CR	0.32	0.15
Mo	0.63	0.40
Cu	0.02	0.21

Heat Treatment

Heat No.	Temp, F	Time, h	Cooling
BCC241	1640±10	4	Water quenched
	1570±10	4	Water quenched
	1240±10	6	Air cooled
	1125±25	40	Furnace cooled
WF-182-1	1100-1150	15	Furnace cooled

(a)Per Certified Materials Test Report.

(b)Per Licensing Document BAW-1500.

Figure 3-1. Reactor Vessel Cross Section Showing Location of Davis-Besse Unit 1 Capsule TE1-B in Davis-Besse Unit 1

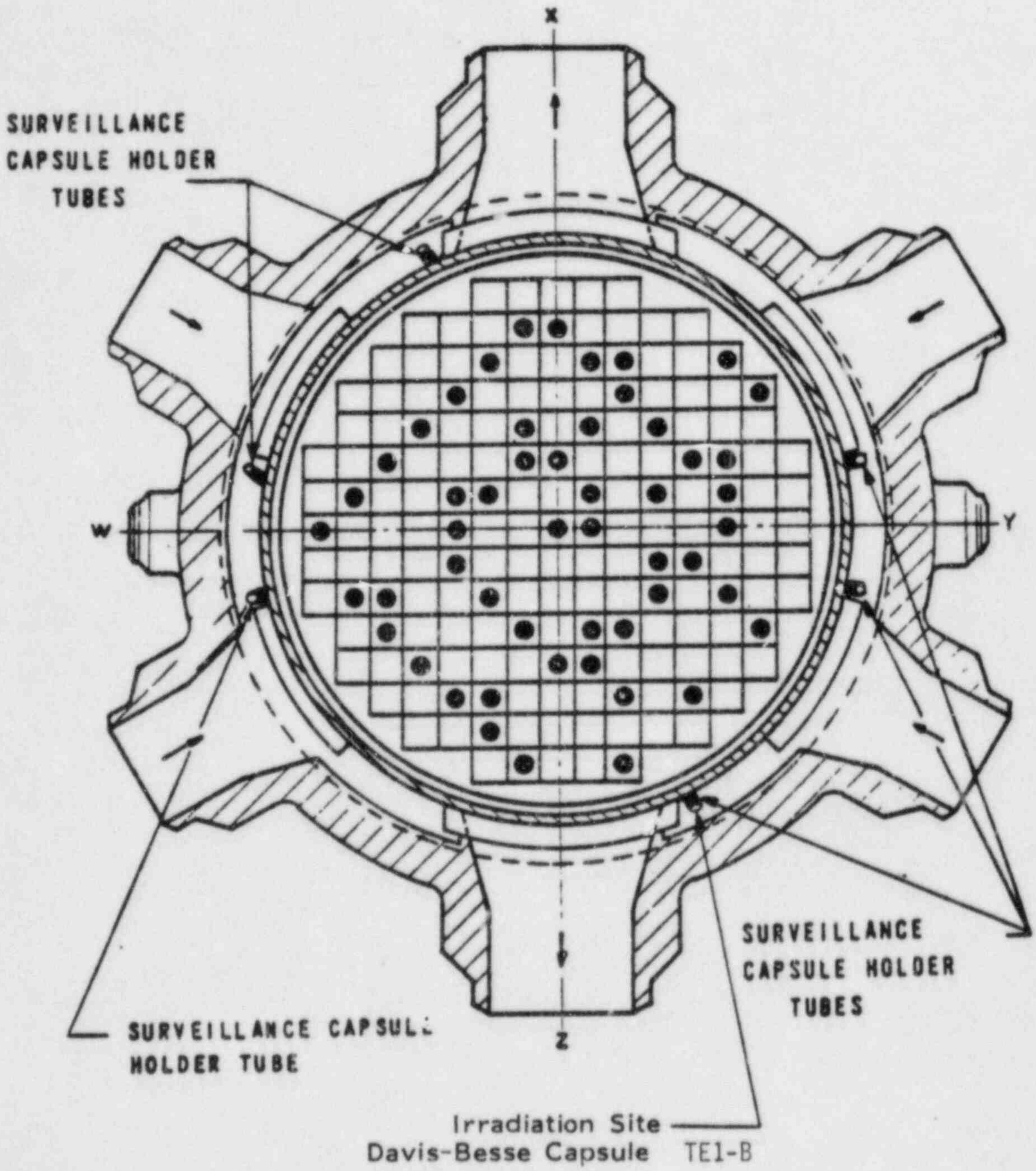

Figure 3-2. Loading Diagram for Test Specimens in TE1-B

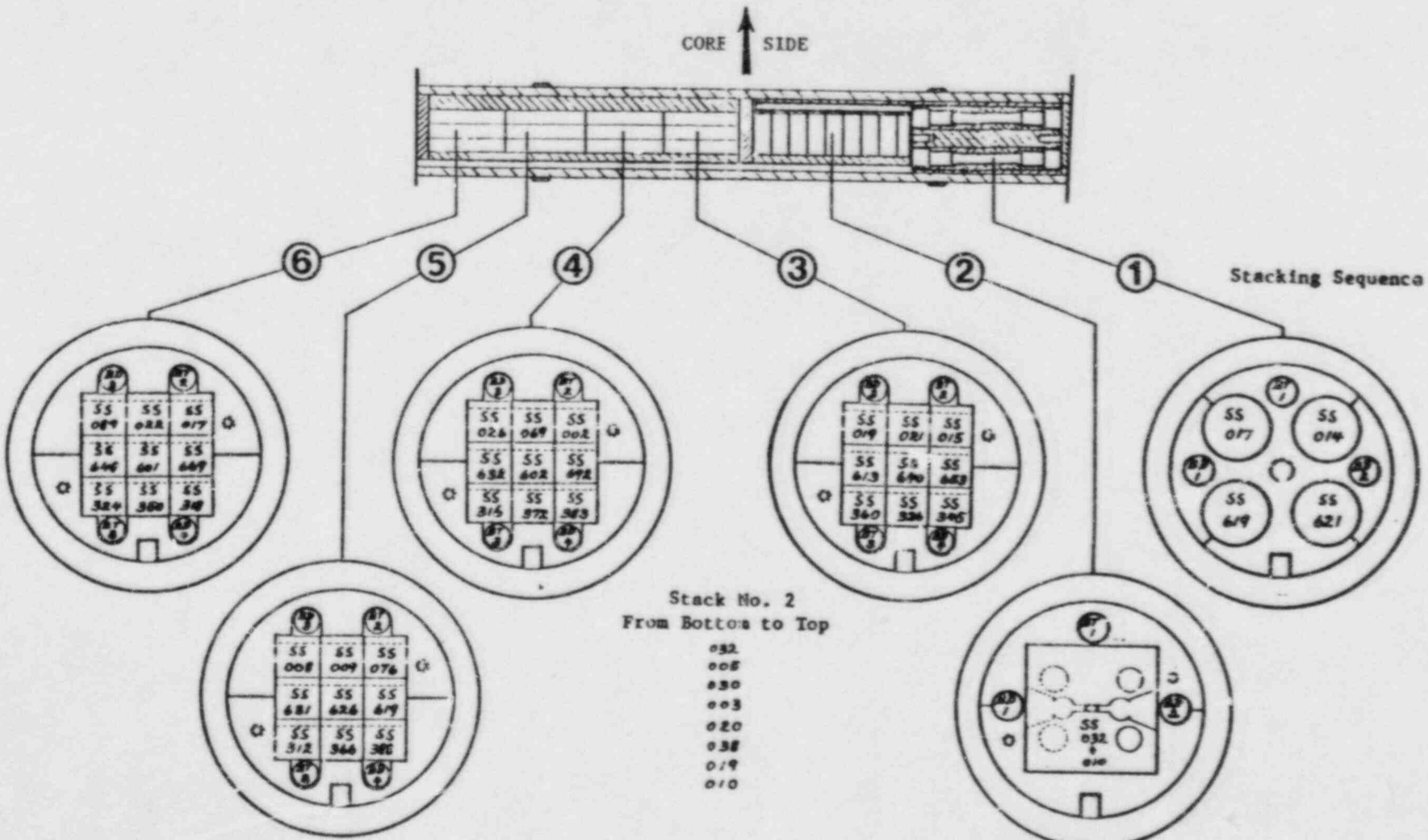

4. PREIRRADIATION TESTS

Unirradiated material was evaluated for two purposes: (1) to establish a baseline of data to which irradiated properties data could be referenced, and (2) to determine those materials properties to the extent practical from available material, as required for compliance with Appendixes G and H to 10 CFR 50.

4.1. Tension Tests

Tension test specimens were fabricated from the reactor vessel shell course forging and weld metal. The subsize specimens were 4.25 inches long with a reduced section 1.750 inches long by 0.357 inch in diameter. They were tested on a 55,000-lb load capacity universal test machine at a crosshead speed of 0.050 inch per minute. A 4-pole extension device with a strain gaged extensometer was used to determine the 0.2% yield point. Test conditions were in accordance with the applicable requirements of ASTM A370-72. For each material type and/or condition, six specimens in groups of three were tested at both room temperature and 580F. The tension-compression load cell used had a certified accuracy of better than ±0.5% of full scale (25,000 lb). All test data for the preirradiation tensile specimens are given in Appendix B.

4.2. Impact Tests

Charpy V-notch impact tests were conducted in accordance with the requirements of ASTM Standard Methods A370-72 and E23-72 on an impact tester certified to meet Watertown standards. Test specimens were of the Charpy V- notch type, which were nominally 0.394 inch square and 2.165 inches long.

Prior to testing, specimens were temperature-controlled in liquid immersion baths, capable of covering the temperature range from -85 to +550F. Specimens were removed from the baths and positioned in the test frame anvil with tongs specifically designed for the purpose. The pendulum was released manually, allowing the specimens to be broken within 5 seconds from their removal from the temperature baths.

Impact test data for the unirradiated baseline reference materials are presented in Appendix C. Tables C-1 through C-3 contain the basis data that are plotted in Figures C-1 through C-3.

4.3. Compact Fracture Tests

The compact fracture specimens fabricated from the weld metal, which were a part of the capsule specimen inventory, were tested by an approved single specimen J-integral testing procedure.[5] The results of the testing of these specimens is reported in a separate report, BAW-1835.[4]

5. POSTIRRADIATION TESTS

5.1. Thermal Monitors

Capsule TE1-B contained three temperature monitor holder tubes, each containing five fusible alloy wires with melting points ranging from 558 to 621F. All the thermal monitors at 558, 580, and 588F had melted while those at the 610F location showed partial melting or slumping; the monitor at the 621F location melted in all three holder tubes. It is therefore assumed that the 610F and 621F monitors were placed in the wrong locations in the holder tubes. From these observations, it was concluded that the capsule had been exposed to a peak temperature in the range of 610 to 621F during the reactor operating period. These peak temperatures are attributed to operating transients that are of short durations and are judged to have insignificant effect on irradiation damage. Short duration operating transients cause the use of thermal monitor wires to be of limited value in determining the maximum steady state operating temperature of the surveillance capsules, however, it is judged that the maximum steady state operating temperature of specimens in the capsule was held within ±25F of the 1/4T vessel thickness location temperature of 577F. It is concluded that the capsule design temperature may have been exceeded during operating transients but not for times and temperatures that would make the capsule data unusable.

5.2. Tension Test Results

The results of the postirradiation tension tests are presented in Table 5-1. Tests were performed on specimens at both room temperature and 580F using the same test procedures and techniques used to test the unirradiated specimens (section 4.1). In general, the ultimate strength and yield strength of the material increased with a corresponding slight decrease in ductility; both effects were the result of neutron radiation damage. The type of behavior observed and the degree to which the material properties changed is within the range of changes to be expected for the radiation environment to which the specimens were exposed.

The results of the preirradiation tension tests are presented in Appendix B.

5.3. Charpy V-Notch Impact Test Results

The test results from the irradiated Charpy V-notch specimens of the reactor vessel beltline material are presented in Tables 5-2 through 5-4 and Figures 5-1 through 5-3. The test procedures and techniques were the same as those used to test the unirradiated specimens (section 4.2). The data show that the material exhibited a sensitivity to irradiation within the values predicted from its chemical composition and the fluence to which it was exposed.

The results of the preirradiation Charpy V-notch impact test are given in Appendix C.

Table 5-1. Tensile Properties of Capsule TE1-B Irradiated Base Metal and Weld Metal

Specimen No.	Test temp, F	Strength, psi Yield	Strength, psi Ult.	Elongation, % Unif	Elongation, % Total	Red'n in area, %
Base Metal, Transverse 5.92×10^{18} n/cm^2 (E > 1 Mev)						
SS-621	76	70,100	91,100	11	26	65
SS-619	580	66,900	87,500	8	21	57
Weld Metal, 5.92×10^{18} n/cm^2 (E > 1 Mev)						
SS-014	76	85,500	100,900	10	16	54
SS-017	580	77,800	93,900	8	15	42

Table 5-2. Charpy Impact Data For Capsule TE1-B Base Metal Irradiated to 5.92E18 n/cm^2 (E >1 MeV)

Specimen No.	Test temp, F	Absorbed energy, ft-lb	Lateral expansion, 10^{-3} in.	Shear fracture, %
SS-669	-47	10.0	7	0
SS-631	-2	29.0	20	0
SS-692	40	50.0	43	10
SS-626	75	62.0	49	30
SS-632	115	93.0	68	80
SS-601	153	98.0	76	70
SS-613	222	107.0	78	100
SS-653	290	112.0	87	100
SS-648	326	117.0	87	100
SS-619	376	115.0	89	100
SS-640	456	118.0	94	100
SS-602	554	102.0	70	100

Table 5-3. Charpy Impact Data For Capsule TE1-B Heat-Affected Zone Metal Irradiated to 5.92E18 n/cm^2 (E > 1 MeV)

Specimen No.	Test temp, F	Absorbed energy, ft-lb	Lateral expansion, 10^{-3} in.	Shear fracture, %
SS-316	-47	26.0	13.0	20
SS-312	-15	52.0	30.0	10
SS-366	-2	66.0	45.0	80
SS-345	40	95.0	62.0	70
SS-383	75	82.0	59.0	70
SS-326	153	104.0	74.0	100
SS-324	222	100.0	78.0	100
SS-350	288	110.0	82.0	100
SS-372	326	117.0	84.0	100
SS-360	376	113.0	86.0	100
SS-318	456	106.0	79.0	100
SS-388	548	103.0	81.0	100

Table 5-4. Irradiated Charpy Impact Data for Capsule TE1-B Weld Metal Irradiated to 5.92E18 n/cm^2 (E > 1 MeV)

Specimen No.	Test temp, F	Absorbed energy, ft-lb	Lateral expansion, 10^{-3} in.	Shear fracture, %
SS-009	-47	9.0	7.0	0
SS-015	40	18.0	16.0	0
SS-002	75	26.0	22.0	20
SS-076	153	36.0	31.0	30
SS-021	222	45.0	37.0	95
SS-006	286	53.0	48.0	100
SS-019	326	57.0	58.0	100
SS-022	376	54.0	43.0	100
SS-017	456	45.0	43.0	100
SS-026	548	52.0	53.0	100

Figure 5-1. Impact Data for Irradiated Shell Forging Material,
Heat BCC241

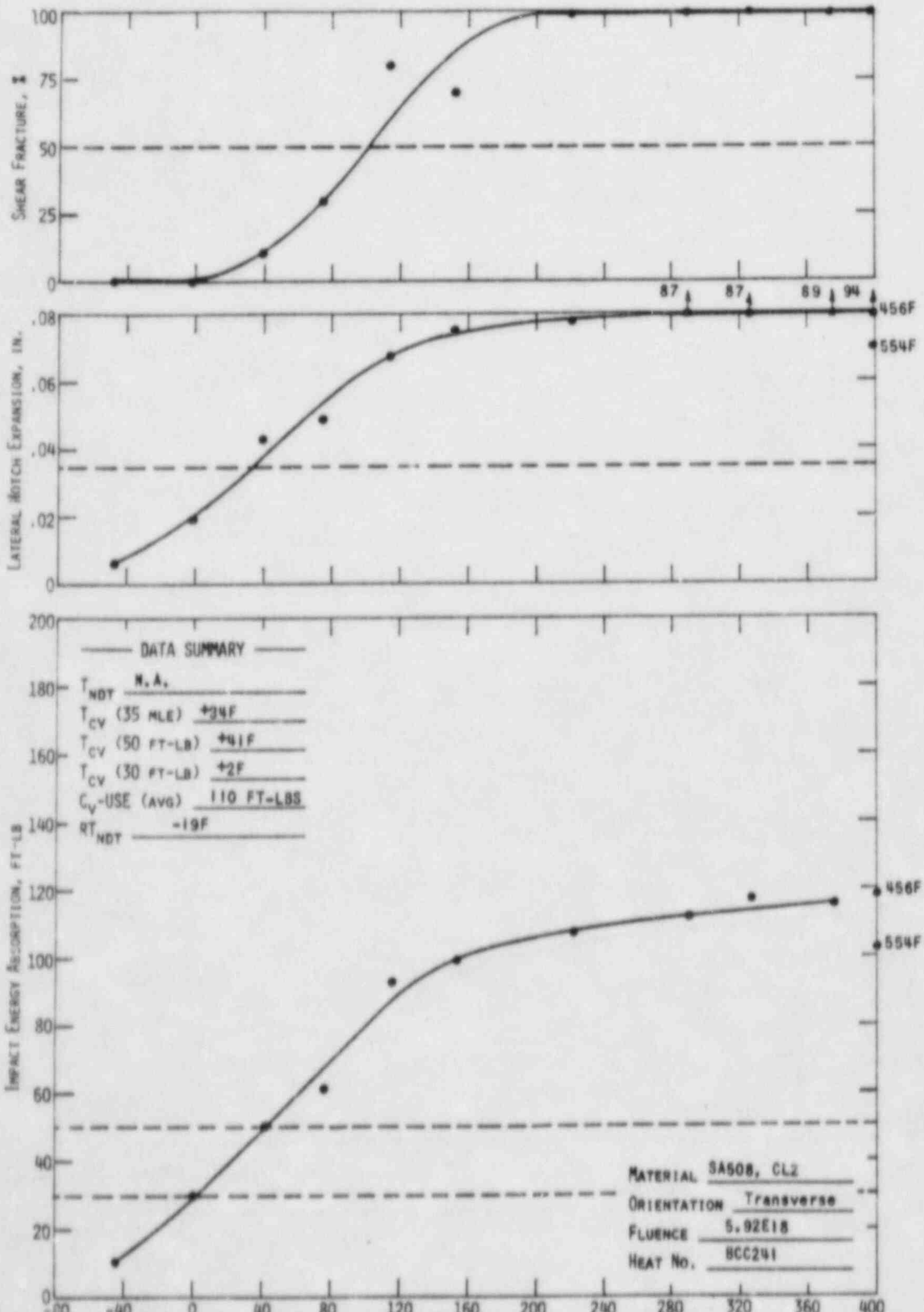

Figure 5-2. Impact Data for Irradiated Shell Forging Material, Heat-Affected Zone, Heat BCC241

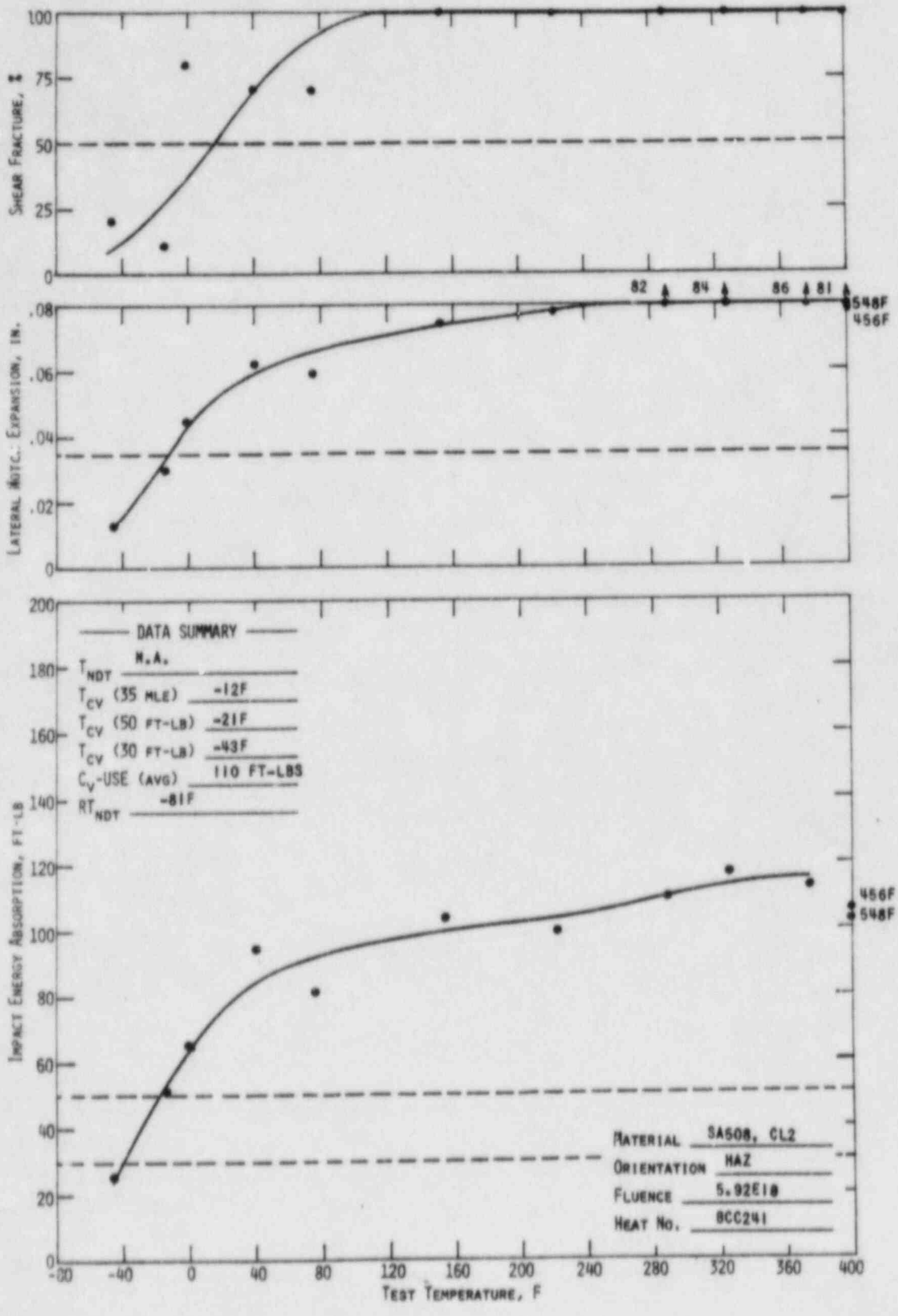

Figure 5-3. Impact Data for Irradiated Weld Metal, WF-182-1

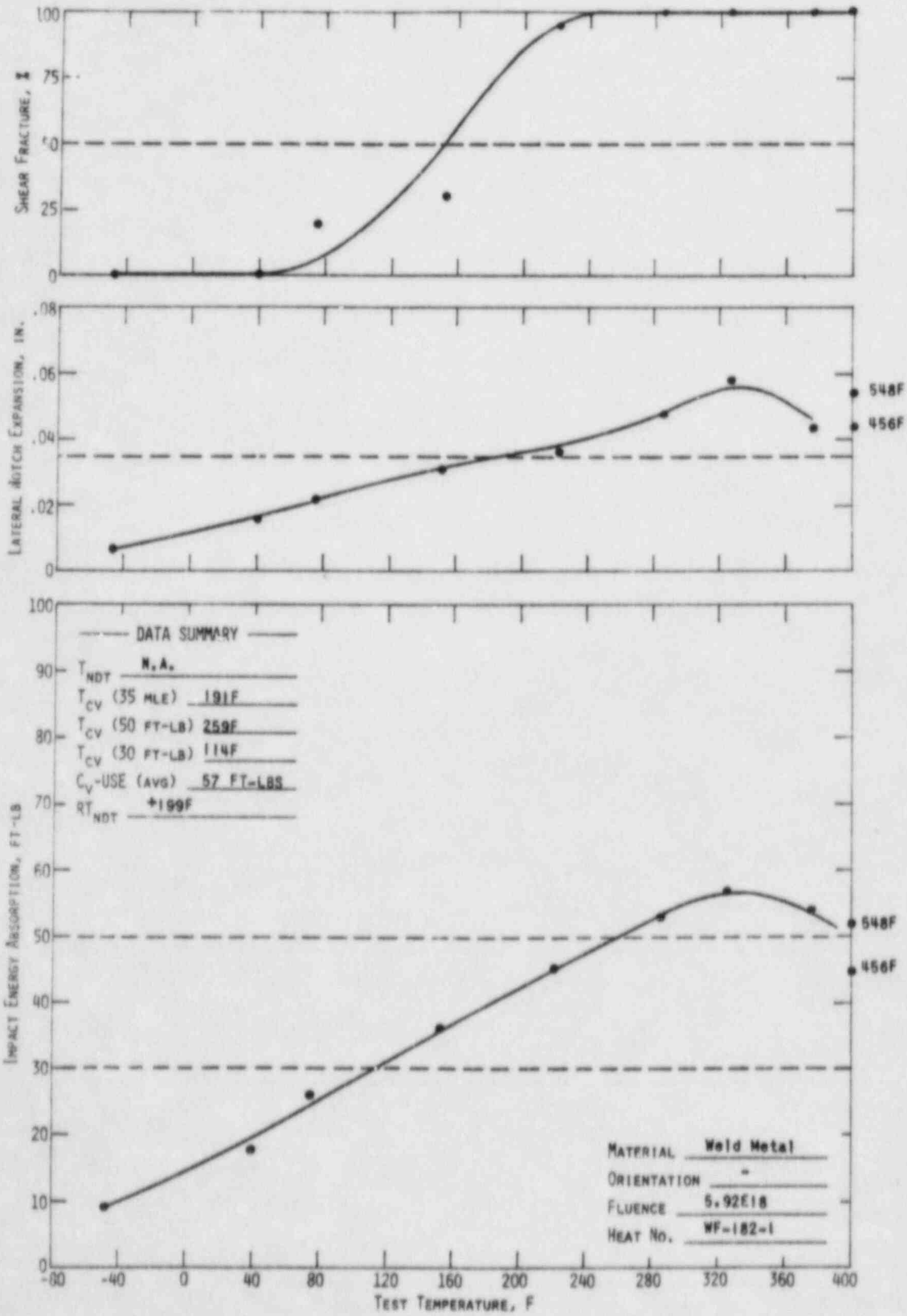

Babcock & Wilcox
a McDermott company

6. NEUTRON DOSIMETRY

6.1. Background

Fluence analysis as a part of the reactor vessel surveillance program has three objectives: (1) determination of maximum fluence at the pressure vessel as a function of reactor operation, (2) prediction of pressure vessel fluence in the future, and (3) determination of the test specimen fluence within the surveillance capsule. Vessel fluence data are used to evaluate changes in the reference transition temperature and upper shelf energy levels, and to establish pressure-temperature operation curves. Test specimen fluence data are used to establish a correlation between changes in material properties and fluence exposure. Fluence data are obtained from calculations based on measured capsule dosimeter activities.

A significant aspect of the surveillance program is to provide a correlation between the neutron fluence above 1 MeV and the radiation-induced property changes noted in the surveillance specimens. To permit such a correlation, activation detectors with reaction thresholds in the energy range of interest were placed in each surveillance capsule. The significant properties of the detectors are given in Tables 6-1 and E-1.

Because of a long half-life (30 years) and effective threshold energies of 0.5 and 1.1 MeV, the measurements of ^{137}Cs production from fission reactions in ^{237}Np (and ^{238}U) are more directly applicable to analytical determinations of the fast neutron fluence (E > 1 MeV) for multiple fuel cycles than are other dosimeter reactions. Other dosimeter reactions are useful as corroborating data for shorter time intervals and/or higher energy fluxes. Short-lived isotope activities are representative of reactor conditions only over the latter portion of the irradiation period (fuel cycle), whereas reactions with a threshold energy > 2 or 3 MeV do not record a significant part of the total fast flux.

The energy-dependent neutron flux is not directly available for activation detectors because the dosimeters register only the integrated effect of neutron flux on the target material as a function of both irradiation time and neutron energy. To obtain an accurate estimate of the average neutron flux incident upon the detector, several parameters must be known: the operating history of the reactor, the energy response of the given detector, and the neutron spectrum at the detector location. Of these parameters, the definition of the neutron spectrum is the most difficult to obtain.

6.2. Vessel Fluence

The maximum fluence (E > 1.0 MeV) in the pressure vessel was determined to be 9.88 (+17) n/cm^2 based on an averge neutron flux of 2.01 (+10) n/cm^2-s for cycles 2 and 3 (Tables 6-2 and 6-3). The location of maximum fluence is assumed to be at the same point at the cladding/vessel interface as for cycle 1: at an elevation of about 110 cm above the lower active fuel boundary and at an azimuthal (peripheral) location of ~11° from a major axis (across flats diameter). Fluence data have been extrapolated to 32 EFPY of operation based on the premise that excore flux is proportional to fast flux that escapes the reactor core (Appendix D). Core escape flux values are available for fuel management analyses of future fuel cycles.

Relative fluence as a function of radial location in the pressure vessel is shown in Figure 6-1. Reactor vessel lead factors (clad interface flux/in-vessel flux) for the T/4, T/2, 3T/4 locations are 1.8, 3.7, and 7.9, respectively. Relative fluence as a function of azimuthal angle is shown in Figure 6-2. A peak occurs at ~11° which roughly corresponds to a corner of the core and to three symmetric capsule locations. Two other capsule locations (including capsule TE1-B) correspond to the azimuthal minimum at ~27°. However, it should be noted that the maximum to minimum flux ratio is only 1.5. Fast neutron flux is increased by ~1.25 in the capsule due to differences in scattering and absorption cross sections between steel and water.

6.3. Capsule Fluence

Fast fluence at the center of the surveillance capsules was calculated to be 5.92 (+18) n/cm^2 (Table 6-4). These data represent average values in the capsule. Capsule TE1-B was located in a upper holder tube position at

~27° off axis and 202 cm from the core axis during cycles 1, 2, and 3 (943 EFPD).

6.4. Uncertainty

1. The estimated uncertainty of the capsule fast flux and fluence values is 15%.
2. The estimated uncertainty of the calculated reactor vessel fluence values is 28%.
3. The estimated uncertainty of the EOL reactor vessel fluence predictions is 30%.

Table 6-1. Surveillance Capsule Detectors

Detector reaction	Effective lower energy limit, MeV	Isotope half-life
$^{54}Fe(n,p)^{54}Mn$	2.5	312.5 days
$^{58}Ni(n,p)^{58}Co$	2.3	70.85 days
$^{238}U(n,f)^{137}Cs$	1.1	30.03 years
$^{237}Np(n,f)^{137}Cs$	0.5	30.03 years

Table 6-2. Reactor Vessel Flux

	Fast flux, n/cm^2-s (E > 1 MeV)				Fast Flux, n/cm^2-s (E > 0.1 MeV)
	Inside surface (max location)	T/4	T/2	3T/4	Inside surface (max location)
Cycle 1[a] (374 EFPD)	1.61 (+10)	8.9 (+9)	4.4 (+9)	2.0 (+9)	3.4(+10)
Cycles 2 & 3[a] (569 EFPD)	2.01 (+10)	1.1 (+10)	5.4 (+9)	2.5 (+9)	--
Cycle 4[b]	2.12 (+10)	1.2 (+10)	5.7 (+9)	2.7 (+9)	--
Cycle 5[b]	1.51 (+10)	8.4 (+9)	4.1 (+9)	1.9 (+9)	--

[a]Calculated.

[b]Predicted.

Table 6-3. Reactor Vessel Fluence Gradient

Cumulative irradiation time	Fast fluence, n/cm^2 (E > 1.0 MeV) Inside surface (max location)	T/4	T/2	3T/4
End of cycle 1 (374 EFPD)	5.19 (+17)	2.9 (+17)	1.4 (+17)	6.6 (+16)
End of cycle 3 (943 EFPD)	1.51 (+18)	8.4 (+17)	4.1 (+17)	1.9 (+17)
End of cycle 4 (3.3 EFPY)	1.98 (+18)	1.1 (+18)	5.4 (+17)	2.5 (+17)
End of cycle 5 (4.4 EFPY)	2.5 (+18)	1.4 (+18)	6.7 (+17)	3.2 (+17)
End of 8 EFPY	4.2 (+18)	2.3 (+18)	1.1 (+18)	5.4 (+17)
End of 15 EFPY	7.6 (+18)	4.2 (+18)	2.0 (+18)	9.6 (+17)
End of 21 EFPY	1.0 (+19)	5.6 (+18)	2.8 (+18)	1.3 (+18)
End of 32 EFPY	1.6 (+19)	8.9 (+18)	4.2 (+18)	2.0 (+18)

Table 6-4. Surveillance Capsule Fluence

	E > 1.0 MeV Flux (n/cm^2-s)	Fluence (n/cm^2)
TE1-F cycle 1 (374 EFPD)	6.08 (+10)	1.96 (+18)
TE1-B cycles 2 & 3 (569 EFPD)	8.06 (+10)	3.96 (+18)
TE1-B cycles 1, 2, and 3 (943 EFPD)		5.92 (+18)

Figure 6-1. Reactor Vessel Flux/Fluence Gradient

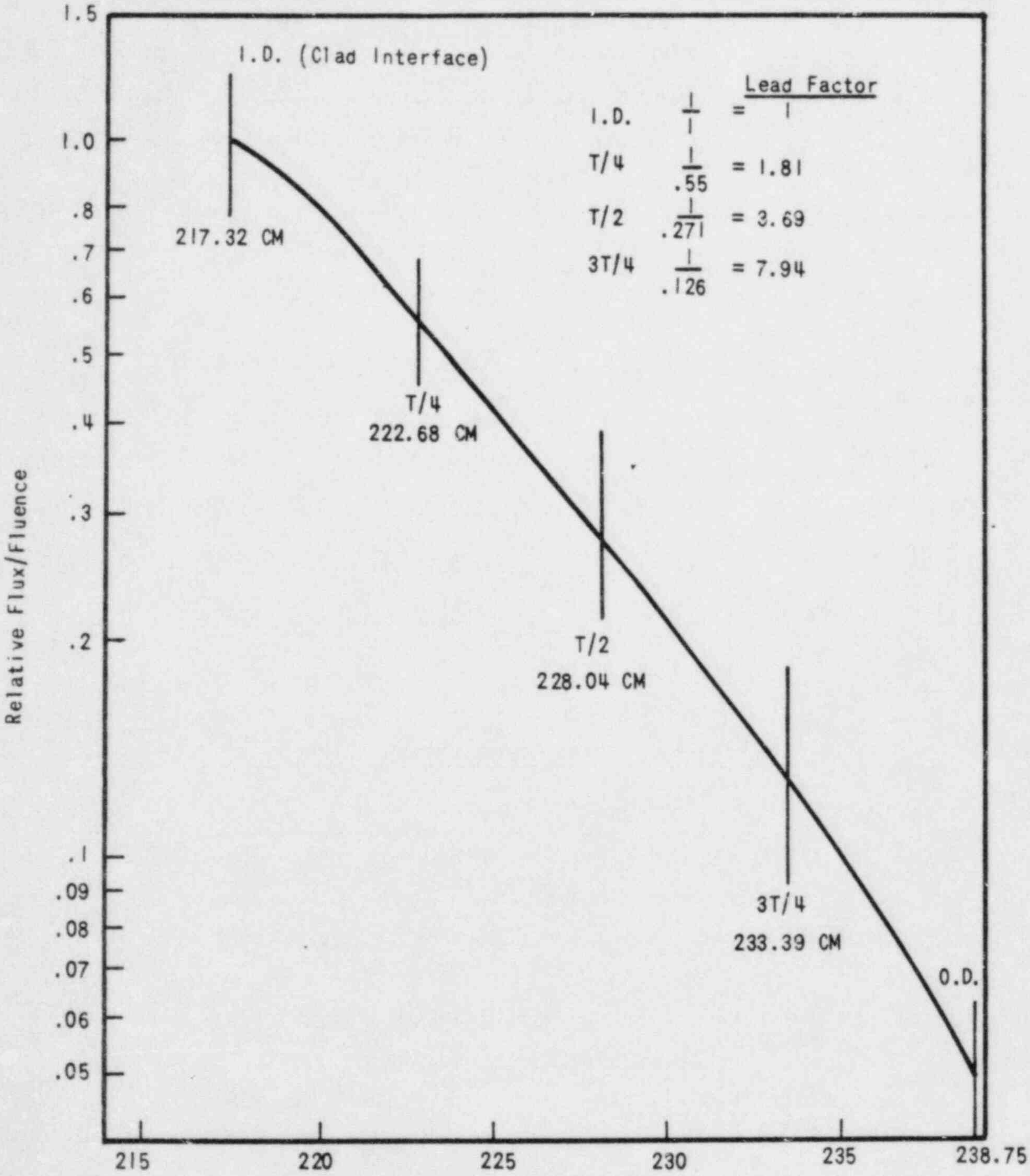

Figure 6-2. Azimuthal Flux/Fluence Gradient Inside Surface of Reactor Vessel

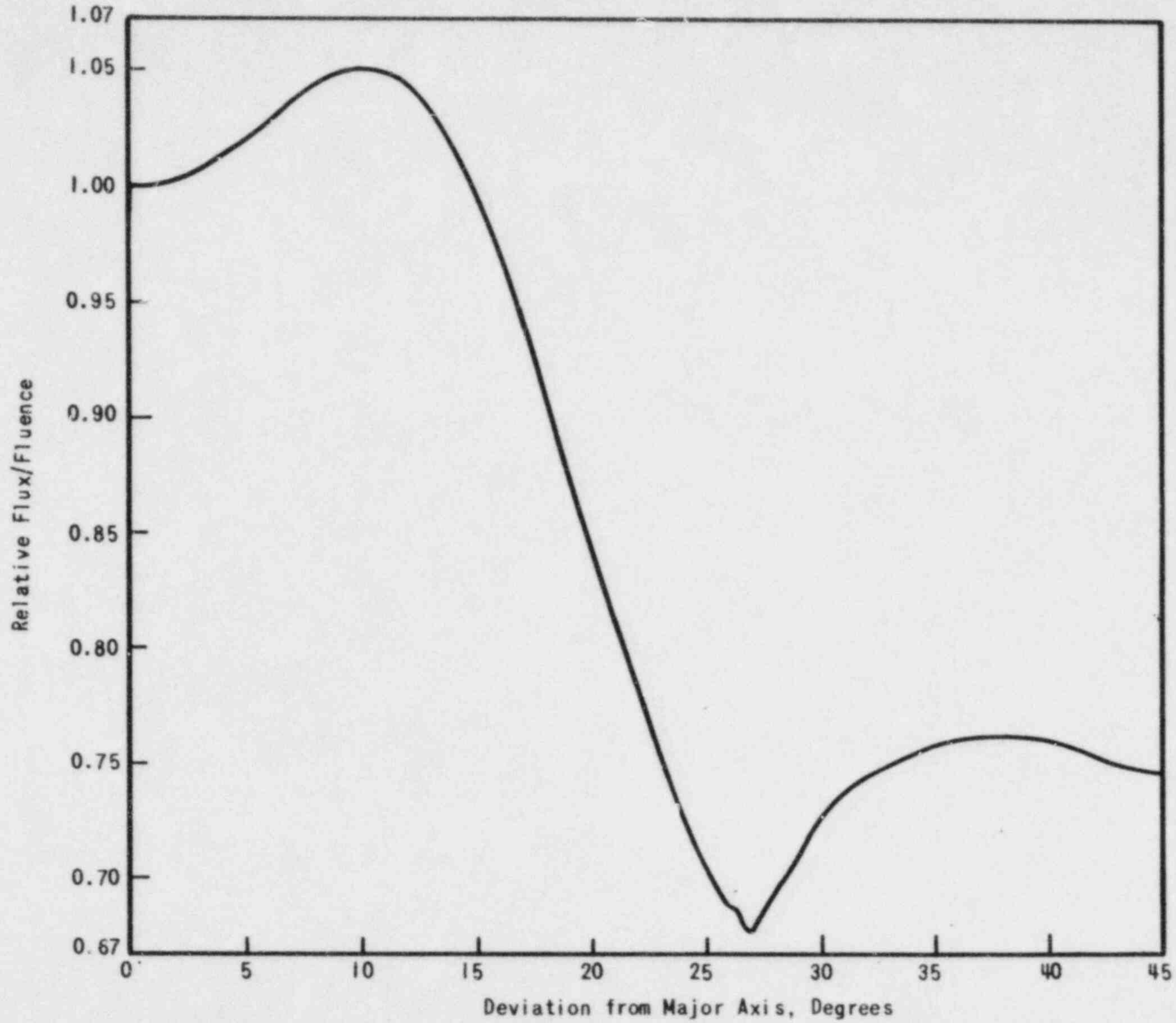

7. DISCUSSION OF CAPSULE RESULTS

7.1. Preirradiation Property Data

A review of the unirradiated properties of the reactor vessel core belt region indicated no significant deviation from expected properties except in the case of the upper shelf properties of the weld metal. Based on the predicted end-of-service peak neutron fluence value at the 1/4T vessel wall location and the copper content of this weld, it was predicted that the end-of-service Charpy upper shelf energy (USE) will be below 50 ft-lb. This weld was selected for inclusion in the surveillance program in accordance with the criteria in effect at the time the program was designed for Davis-Besse Unit 1. The applicable selection criterion was based on the unirradiated properties only.

7.2. Irradiated Property Data

7.2.1. Tensile Properties

Table 7-1 compares irradiated and unirradiated tensile properties. At both room temperature and elevated temperature, the ultimate and yield strength changes in the base metal as a result of irradiation and the corresponding changes in ductility are negligible. There appears to be some strengthening, as indicated by increases in ultimate and yield strength and similar decreases in ductility properties. All changes observed in the base metal are such as to be considered within acceptable limits. The changes at both room temperature and 580F in the properties of the weld metal are greater than those observed for the base metal, indicating a greater sensitivity of the weld metal to irradiation damage. In either case, the changes in tensile properties are insignificant relative to the analysis of the reactor vessel materials at this period in service life.

A comparison of the tensile data from the first capsule (capsule TE1-F) with the corresponding data from the capsule reported in this report is shown in Table 7-2. The currently reported data experienced a fluence that is three times greater than the previous capsule.

The general behavior of the tensile properties as a function of neutron irradiation is an increase in both ultimate and yield strength and a decrease in ductility as measured by both total elongation and reduction of area. The most significant observation from these data is that the weld metal exhibited much greater sensitivity to neutron radiation than the base metal.

7.2.2. Impact Properties

The behavior of the Charpy V-notch impact data is more significant to the calculation of the reactor system's operating limitations. Table 7-3 compares the observed changes in irradiated Charpy impact properties with the predicted changes.

The 50 ft-lb transition temperature shift for the base metal is not in good agreement with the shift that would be predicted according to Regulatory Guide 1.99. The less than ideal comparison may be attributed to the spread in the data of the unirradiated material combined with a minimum of data points to establish the irradiated curve. Under these conditions, the comparison indicates that the estimating curves in RG 1.99 for medium-copper materials and at mid-range fluence levels are conservative for predicting the 50 ft-lb transition temperature shifts.

The 30 ft-lb transition temperature shift for the base metal is not in good agreement with the value predicted according to Regulatory Guide 1.99, although it would be expected that these values would exhibit better agreement when it is considered that a major portion of the data used to develop Regulatory Guide 1.99 was taken at the 30 ft-lb temperature.

The increase in the 35-mil lateral expansion transition temperature is compared with the shift in RT_{NDT} curve data in a manner similar to the comparison made for the 50 ft-lb transition temperature shift. These data show a behavior similar to that observed from the comparison of the observed and predicted 50 ft-lb transition data.

The transition temperature measurements at 30 and 50 ft-lbs for the weld metal are in poor agreement with the predicted shift. This may be attributed to the decrease in upper shelf which caused a larger shift at the 50 ft-lb level than at the 30 ft-lb level. At the 30 ft-lb level the shift is much less than the predicted value which indicates that the estimating curves are conservative for predicting the 30 ft-lb transition temperature shifts.

The data for the decrease in Charpy USE with irradiation did not show good agreement with predicted values for both the base metal and the weld metal. However, the poor comparison of the measured data with the predicted value is not unexpected in view of the lack of data for medium- to high-copper-content materials at low to medium fluence values that were used to develop the estimating curves.

A comparison of the Charpy impact data from the first capsule (capsule TE1-F) with the corresponding data from the capsule reported in this report is shown in Table 7-4. The currently reported data experienced a fluence that is three times greater than the previous capsule.

The base metal exhibited shifts at the 30 ft-lb and 50 ft-lb levels for the latest capsule that were greater than those of the first capsule. The corresponding data for the weld metal showed about a 70% increase at the 50 ft-lb level and for all practical purposes no change at the 30 ft-lb level. This was due to the fact that there was a large decrease in the upper shelf drop which caused a larger shift at the 50 ft-lb level as compared to the 30 ft-lb level.

Both the base metal and the weld metal exhibited further decrease in the upper shelf values. These data confirm that the upper shelf drop for this weld metal does not reach saturation as observed in the results of capsules evaluated by others. This lack of saturation of Charpy USE drop for this weld metal should not be considered indicative of a similar lack of saturation of upper shelf region fracture toughness properties. This relationship must await the testing and evaluation of the data from compact fracture toughness test specimens.

Results from other surveillance capsules also indicate that RT_{NDT} estimating curves have greater inaccuracies than originally thought. These inaccuracies are a function of a number of parameters related to the basic data available at the time the estimating curves were established. Some of these include inaccurate fluence values, poor chemical composition values, and variations in data interpretation. The change in the regulations requiring the shift measurement to be based on the 30 ft-lb value will minimize errors that result from using the 30 ft-lb data base to predict the shift behavior at 50 ft-lbs.

The design curves for predicting the shift will be modified as more data become available; until that time, the design curves for predicting the RT_{NDT} shift as given in Regulatory Guide 1.99 are considered adequate for predicting the RT_{NDT} shift of those materials for which data are not available and will continue to be used to establish the pressure-temperature operational limitations for the irradiated portions of the reactor vessel until the time that new prediction curves are developed and approved.

The lack of good agreement of the change in Charpy USE is further support of the inaccuracy of the prediction curves at the lower fluence values. Although the prediction curves are conservative in that they predict a larger drop in upper shelf than is observed for a given fluence and copper content, the conservatism can unduly restrict the operational limitations. These data support the contention that the USE drop curves will have to be modified as more reliable data become available; until that time the design curves used to predict the decrease in USE of the controlling materials are considered conservative.

Table 7-1. Comparison of Tensile Test Results

	Room temp test		Elevated temp test (580F)	
	Unirr	Irrad	Unirr	Irrad
Base Metal -- BCC-241 Transverse				
Fluence, 10^{18} n/cm^2 (>1 MeV)	0	5.92	0	5.92
Ult. tensile strength, ksi	90.7	91.1	86.3	87.5
0.2% yield strength, ksi	72.3	70.1	64.0	66.9
Elongation, %	28	26	26	21
RA, %	68	65	65	57
Weld Metal -- WF-182-1				
Fluence, 10^{18} n/cm^2 (>1 MeV)	0	5.92	0	5.92
Ult. tensile strength, ksi	85.6	100.9	83.2	93.9
0.2% yield strength, ksi	70.2	85.5	67.6	77.8
Elongation, %	27	16	19	15
RA, %	64	54	50	42

Table 7-2. Summary of Davis-Besse Reactor Vessel Surveillance Capsules Tensile Test Results

Material	Fluence 10^{18} n/cm^2	Test temp, F	Strength, ksi: Ultimate	Strength, ksi: % Δ (*)	Strength, ksi: Yield	Strength, ksi: % Δ (*)	Ductility, %: Total elon.	Ductility, %: % Δ (*)	Ductility, %: R. of A.	Ductility, %: % Δ (*)
Base metal	0	73	90.7	--	72.3	--	28	--	68	--
		580	86.3	--	64.0	--	26	--	65	--
	1.96	70	95.6	+5.4	75.0	+3.7	26	-7.1	66	-2.3
		580	88.8	+2.9	66.3	+3.6	22	-15.4	59	-9.2
	5.92	76	91.1	+0.4	70.1	-3.0	26	-7.1	65	-4.4
		580	87.5	+1.4	66.9	+4.5	21	-19.2	57	-14.0
Weld metal	0	73	85.6	--	70.2	--	27	--	64	--
		580	83.2	--	67.6	--	19	--	50	--
	1.96	70	98.1	+14.6	82.5	+17.5	25	-7.4	58	-9.4
		580	90.0	+8.2	73.1	+8.1	21	+15.8	48	-4.2
	5.92	76	100.9	+17.8	85.5	+21.8	16	-40.7	54	-15.6
		580	93.9	+12.8	77.8	+15.1	15	-21.0	42	-16.0

(*)Change relative to unirradiated.

Table 7-3. Observed Vs Predicted Changes in Irradiated Charpy Impact Properties

Material	Observed	Predicted[a]
Increase in 30 ft-lb trans temp, F		
Base material (BCC-241) Transverse	Neg	43
Heat-affected zone (BCC-241)	57	43
Weld metal (WF-182-1)	125	154
Increase in 50 ft-lb trans temp, F		
Base material (BCC-241)) Transverse	16	43
Heat-affected zone (BCC-241)	36	43
Weld metal (WF-182-1)	194	154
Increase in 35 MLE trans temp, F		
Base material (BCC-241) Transverse	8	43[b]
Heat-affected zone (BCC-241)	33	43[b]
Weld metal (WF-182-1)	158	154[b]
Decrease in Charpy USE, ft-lb		
Base material (BCC-241) Transverse	17	13
Heat-affected zone (BCC-241)	20	13
Weld metal (WF-182-1)	13	23

[a] These values predicted per Regulatory Guide 1.99, Revision 1.

[b] Based on the assumption that MLE as well as 50 ft-lb transition temperature is used to control the shift in RT_{NDT}.

Table 7-4. Summary of Davis-Besse Reactor Vessel Surveillance Capsules Charpy Impact Test Results

		Trans temp increase, F				Decrease in upper shelf energy, ft-lb	
		30 ft-lb		50 ft-lb			
Material	Fluence, 10^{18} n/cm^2	Observ.	Predicted	Observ.	Predicted	Observ.	Predicted
Base metal	1.96	Neg	25	1	25	7	13
	5.92	Neg	43	16	43	17	13
HAZ metal	1.96	43	25	13	25	15	13
	5.92	57	43	36	43	20	13
Weld metal	1.96	127	89	113	89	6	16
	5.92	125	154	194	154	13	23

8. DETERMINATION OF RCPB PRESSURE-TEMPERATURE LIMITS

The pressure-temperature limits of the reactor coolant pressure boundary (RCPB) of Davis-Besse Unit 1 are established in accordance with the requirements of 10 CFR 50, Appendix G. The methods and criteria employed to establish operating pressure and temperature limits are described in topical report BAW-10046.[6] The objective of these limits is to prevent nonductile failure during any normal operating condition, including anticipated operation occurrences and system hydrostatic tests. The loading conditions of interest include the following:

1. Normal operations, including heatup and cooldown.
2. Inservice leak and hydrostatic tests.
3. Reactor core operation.

The major components of the RCPB have been analyzed in accordance with 10 CFR 50, Appendix G. The closure head region, the reactor vessel outlet nozzle, and the beltline region have been identified as the only regions of the reactor vessel (and consequently of the RCPB) that regulate the pressure-temperature limits. Since the closure head region is significantly stressed at relatively low temperatures (due to mechanical loads resulting from bolt preload), this region largely controls the pressure-temperature limits of the first several service periods. The reactor vessel outlet nozzle also affects the pressure-temperature limit curves of the first several service periods. This is due to the high local stresses at the inside corner of the nozzle, which can be two to three times the membrane stresses of the shell. After the first several years of neutron radiation exposure, the RT_{NDT} of the beltline region materials will be high enough that the beltline region of the reactor vessel will start to control the pressure-temperature limits of the RCPB. For the service period for which the limit curves are established, the maximum allowable pressure as a function of fluid temperature is obtained through a point-by-point comparison of the limits imposed by the closure head region, the outlet nozzle, and the beltline region. The maximum allowable pressure is taken to be the lowest of three calculated pressures.

The limit curves for Davis-Besse Unit 1 are based on the predicted values of the adjusted reference temperatures of all the beltline region materials at the end of the fifteenth EFPY. The fifteenth EFPY was selected because it is estimated that the third surveillance capsule will be withdrawn at the end of the refueling cycle when the estimated capsule fluence corresponds to approximately the twenty-first EFPY. The time difference between the withdrawal of the second and third surveillance capsule provides adequate time for re-establishing the operating pressure and temperature limits for the period period of operation between the third and fourth surveillance capsule withdrawals.

The unirradiated impact properties were determined for the surveillance beltline region materials in accordance with 10 CFR 50, Appendixes G and H. For the other beltline region and RCPB materials for which the measured properties are not available, the unirradiated impact properties and residual elements, as originally established for the beltline region materials, are listed in Table A-1. The adjusted reference temperatures are calculated by adding the predicted radiation-induced RT_{NDT} and the unirradiated RT_{NDT}. The predicted ΔRT_{NDT} is calculated using the respective neutron fluence and copper and phosphorus contents. Figure 8-1 illustrates the calculated peak neutron fluence at several locations through the reactor vessel beltline region wall. The supporting information for Figure 8-1 is described in section 6. The neutron fluence values of Figure 8-1 are the predicted fluences that have been demonstrated (section 6) to be conservative. The design curves of Regulatory Guide 1.99* were used to predict the radiation-induced ΔRT_{NDT} values as a function of the material's copper and phosphorus content and neutron fluence.

- - - - -

*Revision 1, April 1977.

The neutron fluences and adjusted RT_{NDT} values of the beltline region materials at the end of the fifteenth full-power year are listed in Table 8-1. The neutron fluences and adjusted RT_{NDT} values are given for the 1/4T and 3/4T vessel wall locations (T = wall thickness). The assumed RT_{NDT} of the closure head region and the outlet nozzle steel forgings is 60F, in accordance with BAW-10046.

Figure 8-2 shows the reactor vessel's pressure-temperature limit curve for normal heatup. This figure also shows the core criticality limits as required by 10 CFR 50, Appendix G. Figures 8-3 and 8-4 show the vessel's pressure-temperature limit curve for normal cooldown and for heatup during inservice leak and hydrostatic tests, respectively. All pressure-temperature limit curves are applicable up to the sixteenth EFPY. Protection against nonductile failure is ensured by maintaining the coolant pressure below the upper limits of the pressure-temperature limit curves. The acceptable pressure and temperature combinations for reactor vessel operation are below and to the right of the limit curve. The reactor is not permitted to go critical until the pressure-temperature combinations are to the right of the criticality limit curve. To establish the pressure-temperature limits for protection against nonductile failure of the RCPB, the limits presented in Figures 8-2 through 8-4 must be adjusted by the pressure differential between the point of system pressure measurement and the pressure on the reactor vessel controlling the limit curves. This is necessary because the reactor vessel is the most limiting component of the RCPB.

Table 8-1. Data for Preparation of Pressure-Temperature Limit Curves for Davis-Besse -- Applicable Through 15 EFPY

Material ident			Weldment location				Chemistry		Neutron fluence at end of 15 EFPY (E > 1 MeV), n/cm²		Radiation-induced RT_{NDT} at end of 15 EFPY, F[c,d]		Adjusted RT_{NDT} at end of 15 EFPY, F	
Heat No.	Type	Beltline region location	Core midplane to weld CL, cm	Location from major axis, degrees	Weld 1/4T location	Unirr RT_{NDT}, F	Copper content, %	Phosphorus content, %	At 1/4T	At 3/4T	At 1/4T	At 3/4T	At 1/4T	At 3/4T
ADB-203	SA508, Cl. 2	Nozzle belt	--	--	--	+50	0.04	0.007	1.0E18	2.3E17	13	6	63	56
AKJ-233	SA508, Cl. 2	Upper shell	--	--	--	+20	0.04	0.004	4.2E18	9.6E17	26	12	46	32
BCC-241	SA508, Cl. 2	Lower shell	--	--	--	+50	0.02	0.011	4.2E18	9.6E17	36	17	86	67
WF-232	Weld	Upper circum seam (ID 9%)	+198	--	No	(+20)[a]	0.18[b]	0.016[b]	--	--	--	--	--	--
WF-233	Weld	Upper circum seam (OD 91%)	+198	--	Yes	(+20)[a]	0.29[b]	0.021[b]	1.0E18	2.3E17	100	48	120	68
WF-182-1	Weld	Mid circum seam (100%)	-24	--	Yes	+2	0.24[b]	0.014[b]	4.2E18	9.6E18	149	71	151	73
WF-232	Weld	Lower circum seam (ID 12%)	-247	--	No	(+20)[a]	0.18[b]	0.016[b]	--	--	--	--	--	--
WF-233	Weld	Lower circum seam (OD 88%)	-247	--	Yes	(+20)[a]	0.29[b]	0.021[b]	5.1E15	1.1E15	6	3	26	23

(a)Per BAW-10046A, Rev. 1, July 1977.

(b)Per BAW-1799, July 1983.

(c)Per Regulatory Guide 1.99, Rev. 1, April 1977.

(d)Regulatory Guide 1.99 not valid for shifts less than 50F.

Figure 8-1. Predicted Fast Neutron Fluences at Various Locations Through Reactor Vessel Wall for First 15 EFPY -- Davis-Besse 1

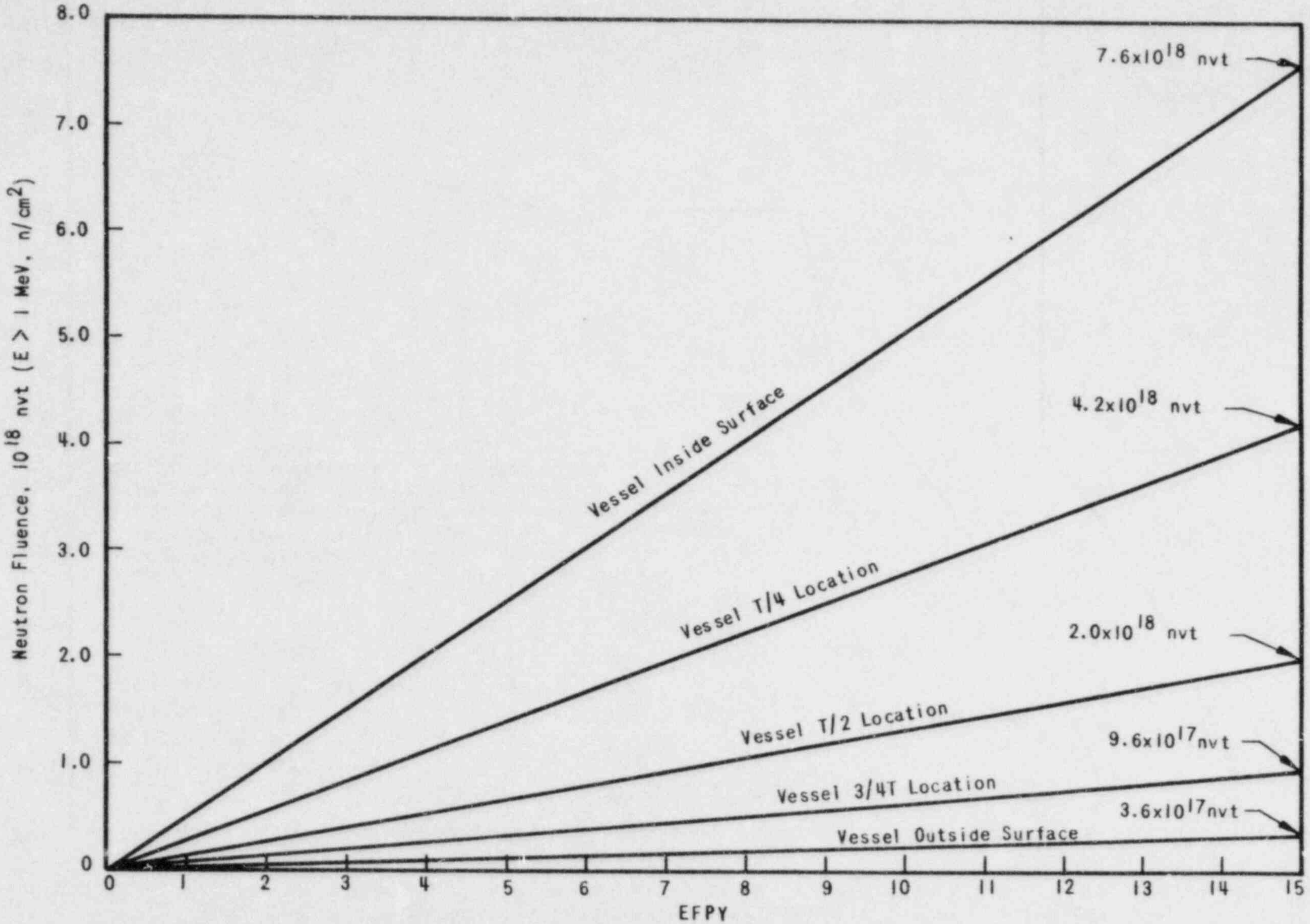

Figure 8-2. Reactor Vessel Pressure-Temperature Limit Curves for Normal Operation -- Heatup Applicable for First 15 EFPY

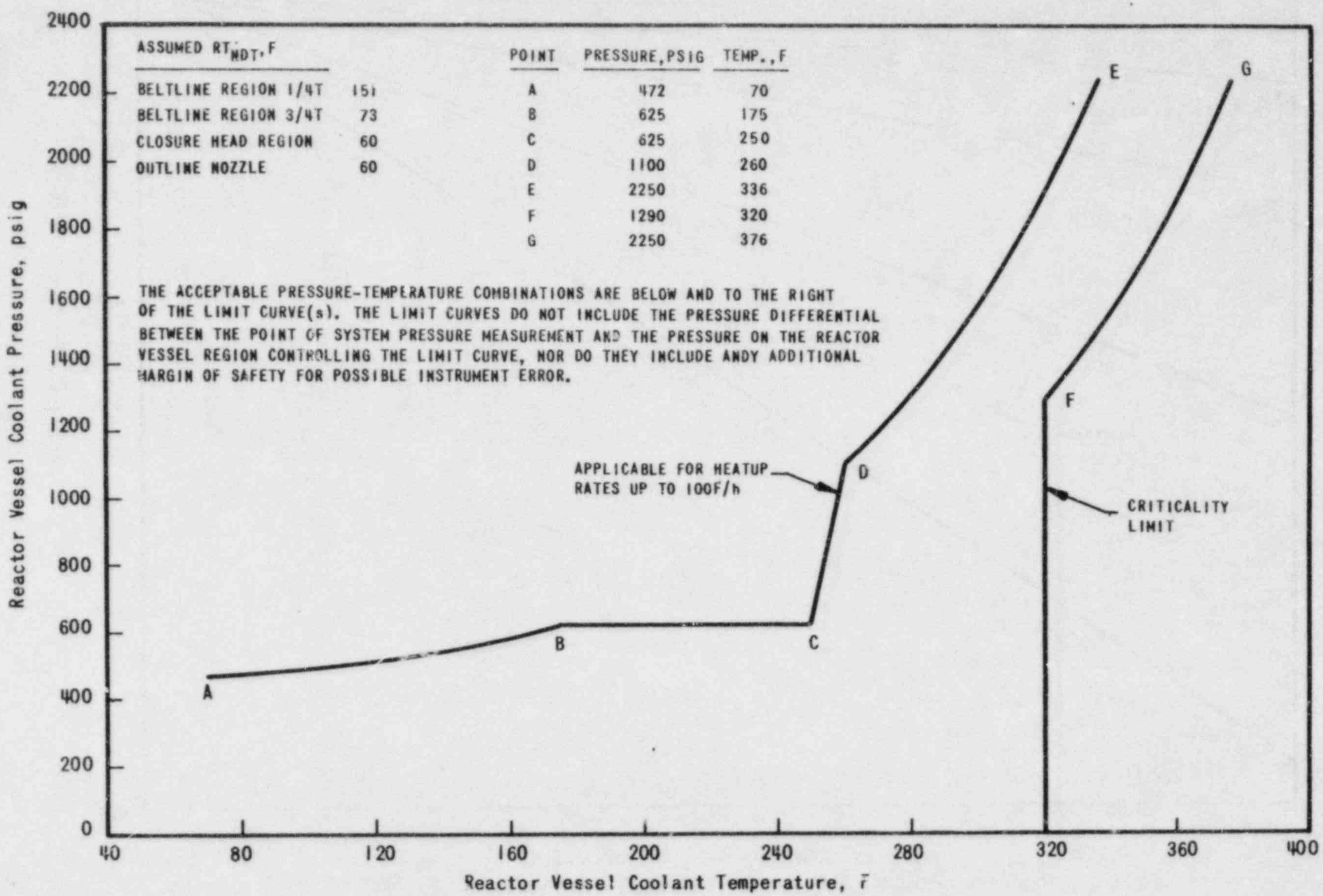

Figure 8-3. Reactor Vessel Pressure-Temperature Limit Curve for Normal Operation -- Cooldown Applicable for First 15 EFPY

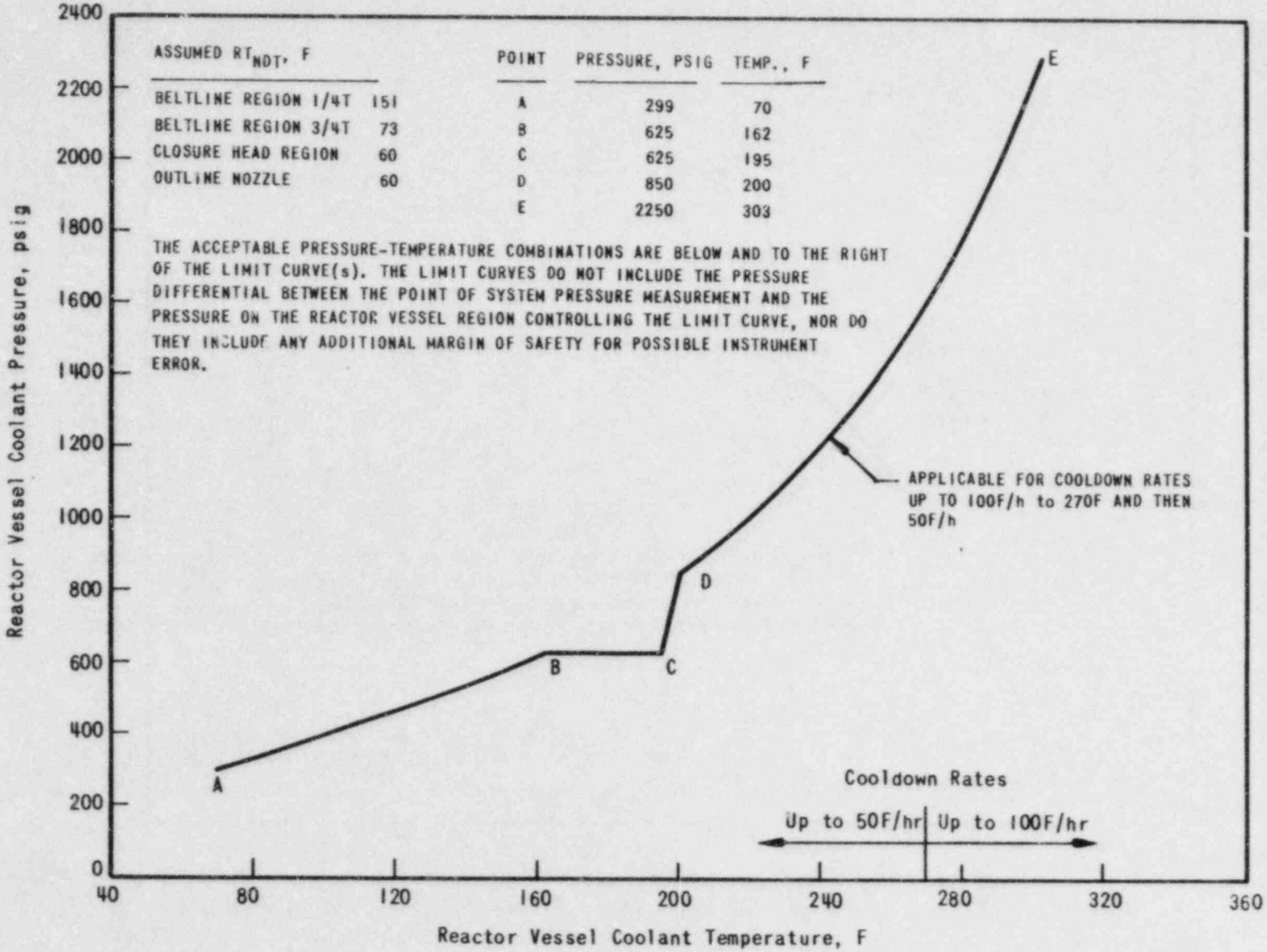

Figure 8-4. Reactor Vessel Pressure-Temperature Limit Curve for Inservice Leak and Hydrostatic Tests, Applicable for First 15 EFPY

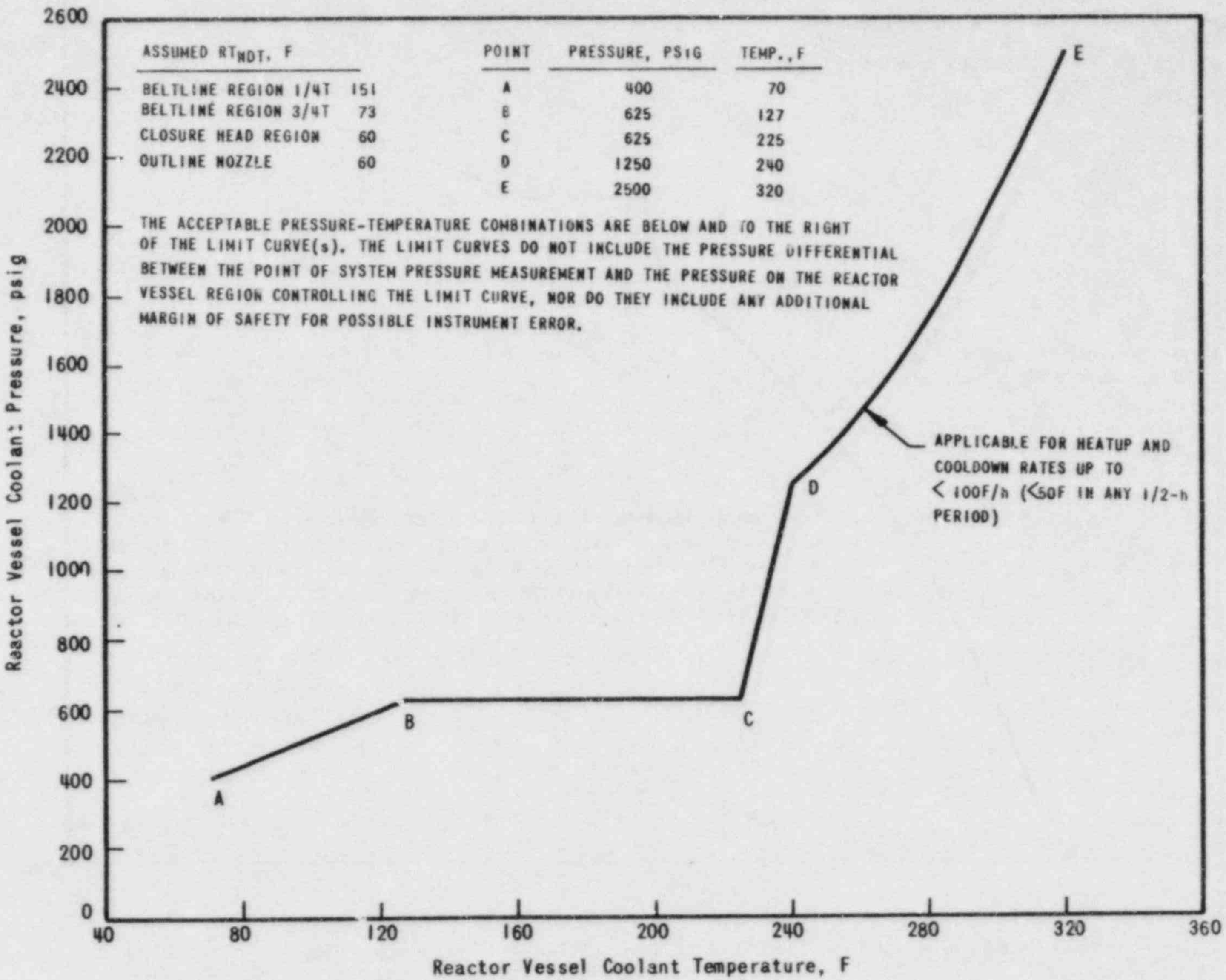

9. SUMMARY OF RESULTS

The analysis of the reactor vessel material contained in the second surveillance capsule, TE1-B, removed for evaluation as part of the Davis-Besse Unit 1 Reactor Vessel Surveillance Program, led to the following conclusions:

1. The capsule received an average fast fluence of 5.92×10^{18} n/cm^2 (E > 1.0 MeV). The predicted fast fluence for the reactor vessel T/4 location at the end of the third fuel cycle is 8.4×10^{17} n/cm^2 (E > 1 MeV).

2. The fast fluence of 5.92×10^{18} n/cm^2 (E > 1 MeV) increased the RT_{NDT} of the capsule reactor vessel core region shell materials a maximum of 125F.

3. Based on the calculated fast flux at the vessel wall, an 80% load factor and the planned fuel management, the projected fast fluence that the Davis-Besse Unit 1 reactor pressure vessel will receive in 40 calendar years' operation is 1.6×10^{19} n/cm^2 (E > 1 MeV).

4. The increase in the RT_{NDT} for the base plate material was not in good agreement with that predicted by the currently used design curves of RT_{NDT} versus fluence, but the prediction techniques are conservative.

5. The increase in the RT_{NDT} for the weld metal was not in good agreement with that predicted by the currently used design curves of RT_{NDT} versus fluence but the prediction techniques are conservative.

6. The current techniques used to predict the change in weld metal Charpy upper shelf properties due to irradiation are conservative.

7. The analysis of the neutron dosimeters demonstrated that the analytical techniques used to predict the neutron flux and fluence were accurate.

8. The capsule design operating temperature may have been exceeded during operating transients but not for times and temperatures that would make the capsule data unusable.

10. SURVEILLANCE CAPSULE REMOVAL SCHEDULE

Based on the postirradiation test results of capsule TE1-B, the following schedule is recommended for examination of the remaining capsules in the Davis-Besse Unit 1 RVSP:

Evaluation schedule[(a)]

Capsule ID	Est. capsule fluence, 10^{19} n/cm^2	Est. vessel fluence, 10^{19} n/cm^2 Surface	Est. vessel fluence, 10^{19} n/cm^2 1/4T	Est. date data available[(b)]
TE1-A	1.1	0.20	0.11	1985
TE1-C	1.6	0.32	0.17	1988
TE1-D[(c)]	1.5	0.44	0.23	1991
TE1-E[(d)]	1.5	0.62	0.32	1996

[(a)] In accordance with BAW-10100A and ASTM E 185-79 as modified by BAW-1543, Rev. 2.

[(b)] Estimated date based on 0.8 plant operation factor.

[(c)] Capsules contain weld metal compact fracture toughness specimens.

[(d)] Capsules designated as standbys and may not be evaluated when removed.

11. CERTIFICATION

The specimens were tested, and the data obtained from Davis-Besse Nuclear Power Station Unit 1 surveillance capsule TE1-B were evaluated using accepted techniques and established standard methods and procedures in accordance with the requirements of 10 CFR 50, Appendixes G and H.

HWarner for 7-11-84

A. L. Lowe, Jr., P.E. Date
Project Technical Manager

This report has been reviewed for technical content and accuracy.

L B Gross 7/11/84

L. B. Gross, P.E. Date
Materials and Chemical
Engineering Services

APPENDIX A

Reactor Vessel Surveillance Program --
Background Data and Information

1. Material Selection Data

The data used to select the materials for the specimens in the surveillance program, in accordance with E-185-73, are shown in Table A-1. The locations of these materials within the reactor vessel are shown in Figures A-1 and A-2.

2. Definition of Beltline Region

The beltline region of Davis-Besse Unit 1 was defined in accordance with the data given in BAW-10100A.

3. Capsule Identification

The capsules used in the Davis-Besse Unit 1 surveillance program are identified below by identification number, type, and location.

Capsule Cross Reference Data

Number	Type	Location
TE1-A	III	Upper
TE1-B	IV	Lower
TE1-C	III	Upper
TE1-D	IV	Lower
TE1-E	III	Upper
TE1-F	IV	Lower

4. Specimens for Determining Material Caseline Properties

See Table A-2.

5. Specimens per Surveillance Capsule

See Tables A-3 and A-4.

Table A-1. Unirradiated Impact Properties and Residual Element Content Data of Beltline Region Materials Used for Selection of Surveillance Program Materials -- Davis-Besse Unit 1

Material ident, heat No.	Material type	Beltline region location	Distance, core midplane to weld centerline, cm	Drop wt, T_{NDT}, F	Charpy data, CVN: Longitudinal At 10F ft-lb	Charpy data, CVN: Transverse 50 ft-lb, F	Charpy data, CVN: Transverse 35 MLE, F	Charpy data, CVN: Transverse USE, ft-lb	RT_{NDT}, F	Chemistry, %(a) Cu	Chemistry, %(a) P	Chemistry, %(a) S	Chemistry, %(a) Ni
ADB-203	SA508, Cl 2	Nozzle belt	--	50	--	61	--	134	50	0.04	0.007	0.009	--
AKJ-233	SA508, Cl 2	Upper shell B	--	20	136,179,130 107,96,81	30	--	144	20	0.04	0.004	0.006	--
BCC-241	SA508, Cl 2	Lower shell A	--	50	60,62,47 47,62,59	27	--	118	50	0.02	0.011	0.011	--
WF-232	Weld	Circum seam upper (9% ID)	+198	--	25,31,35	--	--	--	--	0.14	0.011	0.007	--
WF-233	Weld	Circum seam upper (91% OD)	+198	--	43,30,26	--	--	--	--	0.22	0.015	0.016	--
WF-182-1	Weld	Circum seam middle	-24	-20	36,33,44	62	--	81	2	0.18	0.014	0.015	--
WF-232	Weld	Circum seam lower (12% ID)	-247	--	25,31,35	--	--	--	--	0.14	0.011	0.007	--
WF-233	Weld	Circum seam lower (88% OD)	-247	--	43,30,26	--	--	--	--	0.22	0.015	0.016	--

Table A-2. Test Specimens for Determining Material Baseline Properties

Material description	No. of test specimens			
	Tension			
	70F	600F[a]	CVN impact	Compact-fracture[b]
Heat SS				
Base metal				
Transverse direction	3	3	15	--
Longitudinal direction	3	3	15	--
Heat-affected zone (HAZ)				
Transverse direction	3	3	15	--
Longitudinal direction	3	3	15	--
Total	12	12	60	--
Heat TT				
Base metal				
Transverse direction	3	3	15	--
Longitudinal direction	3	3	15	--
Heat-affected zone (HAZ)				
Transverse direction	3	3	15	--
Longitudinal direction	3	3	15	--
Total	12	12	60	--
Weld metal				
Longitudinal direction	3	3	15	8 1/2 TCT 4 1 TCT

(a)Test temperature to be the same as irradiation temperature.

(b)Test temperature to be determined from shift in impact transition curves after irradiation exposure.

Table A-3. Specimens in Upper Surveillance Capsules (Designation A, C, and E)

Material description	No. of test specimens: Tension	CVN impact
Weld metal	2	12
Weld, HAZ		
Heat SS, transverse	--	12
Heat TT, transverse	--	6
Base metal		
Heat SS, transverse	2	12
Heat TT, transverse	--	6
Correlation material	--	6
Total per capsule	4	54

Table A-4. Specimens in Lower Surveillance Capsules (Designations B, D, and F)

Material description	No. of test specimens: Tension	CVN impact	1/2 T compact fracture[a]
Weld metal	2	12	8
Weld, HAZ			
Heat SS, transverse	--	12	--
Base metal			
Heat SS, transverse	2	12	--
Total per capsule	4	36	8

[a]Compact fracture toughness specimens precracked per ASTM E399-72.

Figure A-1. Location and Identification of Materials Used in Fabrication of Reactor Pressure Vessel

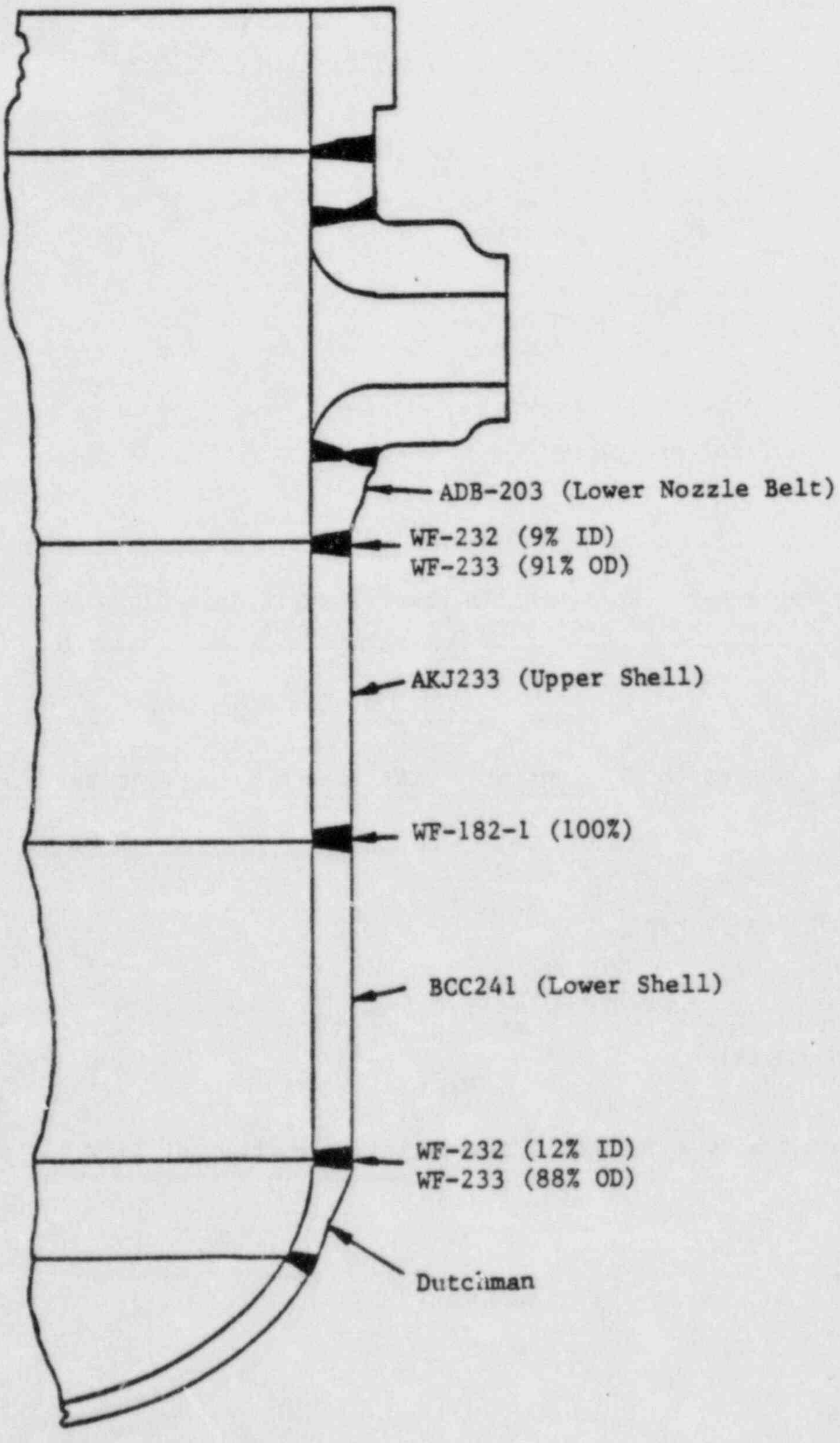

APPENDIX B

Preirradiation Tensile Data

Table B-1. Preirradiation Tensile Properties for Base Metal Heat No. BCC241

Specimen No.	Test temp, F	Strength, psi		Elongation, %		Red'n of area, %
		Yield	Ultimate	Uniform	Total	
SS-601	73	75.6	91.9	12.7	27.0	67.3
SS-603	73	69.4	90.0	13.1	27.2	67.0
SS-604	73	71.9	90.3	13.0	28.8	71.1
Mean	73	72.3	90.7	12.9	27.7	68.5
Std dev'n	73	3.12	1.02	0.21	0.99	2.29
SS-606	580	64.4	86.3	14.4	25.7	65.4
SS-611	580	64.4	86.3	13.6	26.0	63.7
SS-615	578	63.1	86.3	16.3	25.5	67.0
Mean	580	64.0	86.3	14.8	25.7	65.4
Std dev'n	580	0.75	0	1.39	0.25	1.65

Table B-2. Preirradiation Tensile Properties for Weld Metal, WF-182-1

Specimen No.	Test temp, F	Strength, psi		Elongation, %		Red'n of area, %
		Yield	Ultimate	Uniform	Total	
SS-003	73	70.6	85.6	14.8	26.0	63.7
SS-007	73	69.7	85.6	15.4	27.3	64.7
Mean	73	70.2	85.6	15.1	26.7	64.2
Std dev'n	73	0.64	0	0.42	0.92	0.71
SS-009	582	64.4	80.6	14.8	20.0	50.1
SS-015	582	67.8	83.1	11.4	17.4	49.7
SS-016	579	770.6	85.9	12.5	18.9	50.9
Mean	580	67.6	83.2	12.9	18.8	50.2
Std dev'n	580	3.10	2.65	1.73	1.31	0.61

APPENDIX C

Preirradiation Charpy Impact Data

Table C-1. Preirradiation Charpy Impact Data for Shell Forging Material -- Transverse Orientation, Heat BCC-241

Specimen No.	Test temp, F	Absorbed energy, ft-lb	Lateral expansion, 10^{-3} in.	Shear fracture, %
SS-616	-79	5.5	10	0
SS-636	-40	17.5	14	0
SS-609	-2	19.5	18	0
SS-617	0	16.5	16	0
SS-621	+21	39.0	33	2
SS-666	+40	53.0	45	15
SS-667	+40	73.0	57	20
SS-672	+40	88.0	69	60
SS-643	+70	76.0	60	25
SS-646	+70	87.0	70	25
SS-652	+74	109.0	79	85
SS-627	+106	99.0	74	80
SS-663	+130	111.5	85	90
SS-686	+171	120.0	88	100
SS-656	+213	128.5	92	100
SS-658	+278	116.0	89	100
SS-681	+338	113.5	88	100
SS-630	+585	113.0	83	100

Table C-2. Preirradiation Charpy Impact Data for Shell Forging Material -- Heat-Affected Zone, Heat BCC-241

Specimen No.	Test temp, F	Absorbed energy, ft-lb	Lateral expansion, 10^{-3} in.	Shear fracture, %
SS-331	-120	27.0	19	0
SS-307	-80	30.5	16	0
SS-309	-80	60.0	36	0
SS-310	-80	28.0	17	2
SS-325	-59	67.0	37	20
SS-346	-40	56.0	31	10
SS-320	-20	62.0	37	25
SS-337	-20	94.0	54	30
SS-341	-2	97.5	57	60
SS-329	+40	114.5	69	40
SS-305	+74	133.0	76	90
SS-333	+106	135.5	88	100
SS-304	+130	110.5	77	100
SS-315	+176	138.5	82	100
SS-335	+223	110.0	79	100
SS-343	+338	112.0	83	100
SS-322	+406	135.5	84	100
SS-348	+578	101.0	78	100

Table C-3. Preirradiation Charpy Impact Data for Weld Metal, WF-182-1

Specimen No.	Test temp, F	Absorbed energy, ft-lb	Lateral expansion, 10^{-3} in.	Shear fracture, %
SS-046	-80	15.5	16	0
SS-060	-40	16.0	15	2
SS-077	-2	37.5	35	10
SS-084	-2	28.0	27	25
SS-053	0	33.0	29	20
SS-055	0	33.5	29	15
SS-027	+40	40.0	40	50
SS-028	+40	40.0	38	35
SS-029	+40	37.5	34	15
SS-071	+70	45.5	44	50
SS-081	+70	58.0	55	70
SS-092	+74	55.0	56	75
SS-056	+130	70.5	64	100
SS-067	+145	36.5	35	40
SS-036	+169	69.5	64	100
SS-063	+223	72.5	71	100
SS-085	+228	66.5	65	100
SS-016	+338	72.0	70	100
SS-040	+583	68.5	72	100

Figure C-1. Impact Data for Unirradiated Shell Forging Material, Heat BCC-241

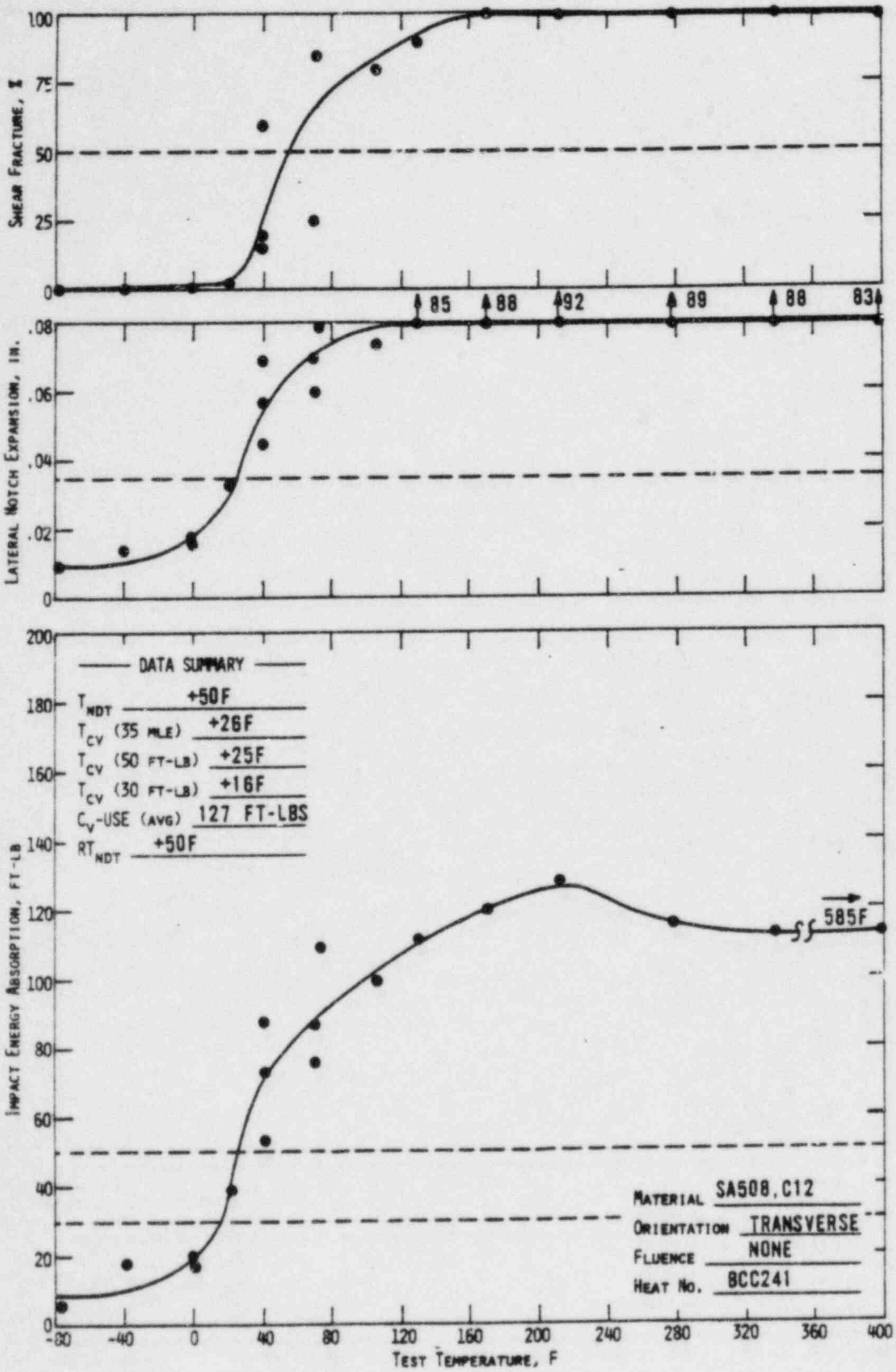

Figure C-2. Impact Data for Unirradiated Shell Forging Material, Heat-Affected Zone, Heat BCC-241

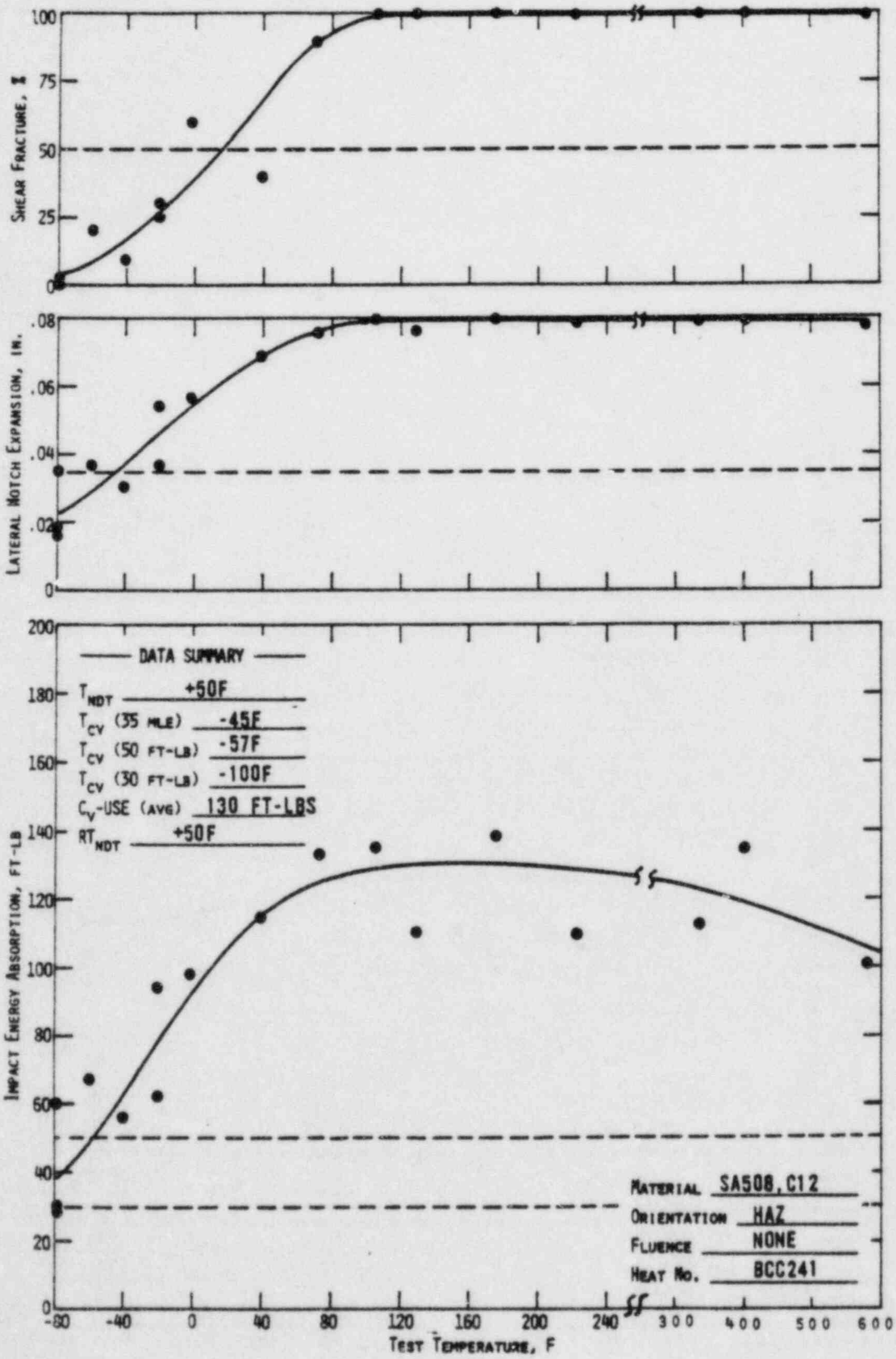

Figure C-3. Impact Data for Unirradiated Weld Metal, WF-182-1

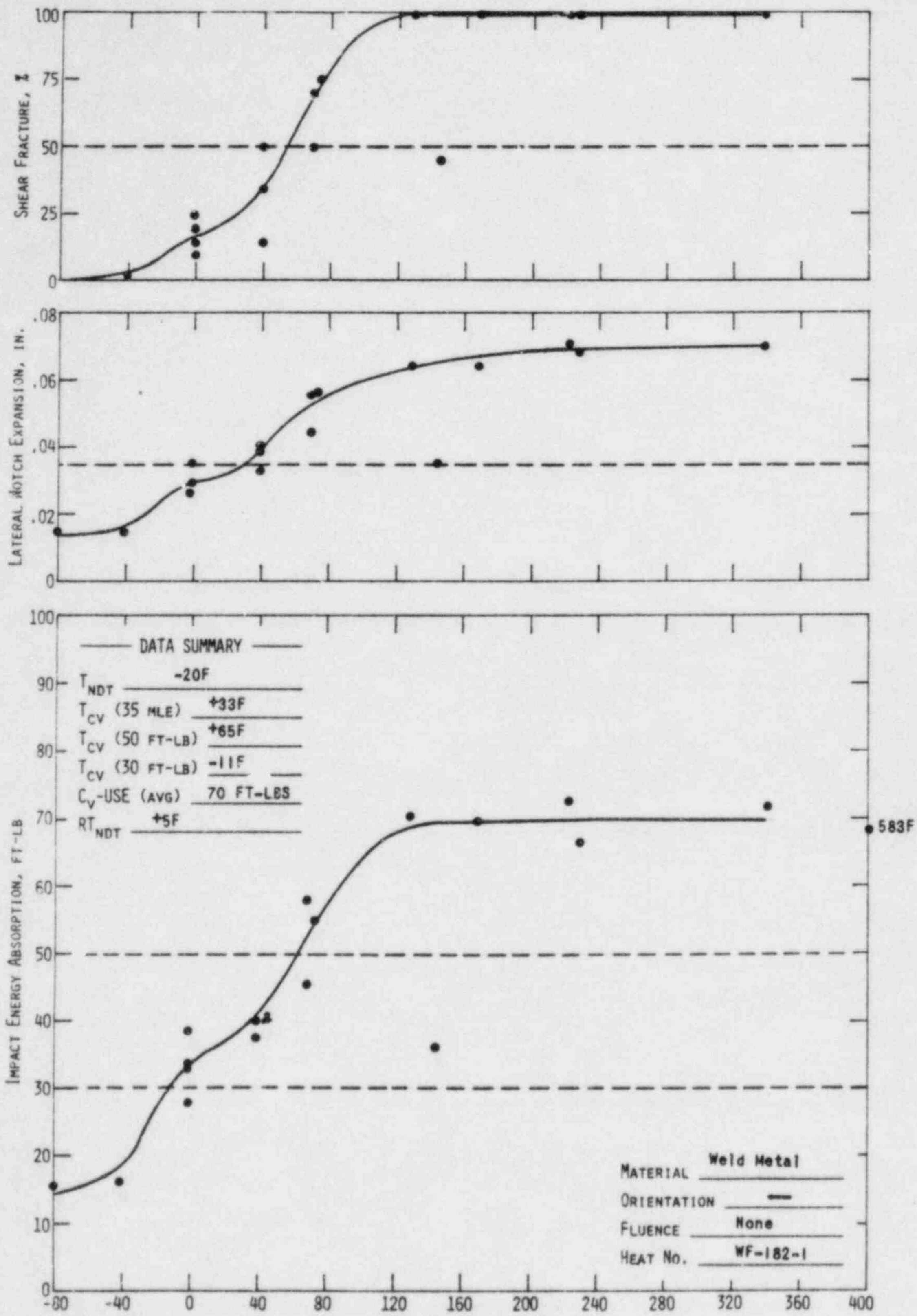

APPENDIX D

Fluence Analysis Procedures

Analytical Method

Neutron flux values at the capsule position are caculated from measured capsule dosimeter activities using the following equation:

$$\emptyset_{2+3} = 3.7 \times 10^4 \frac{A_n}{Nf_i \bar{\sigma} PI} (A_T - A_1 e^{-\lambda_i t_1})$$

$$= 6.14414 \times 10^4 \frac{A_n}{f_i \bar{\sigma} PI} (A_T - A_1 e^{-\lambda_i t_1})$$

where

$$PI = \sum_{j=1}^{M} F_j(1 - e^{-\lambda_i t_j}) e^{-\lambda_i (T - \tau_j)}$$ (Known as: Power Integral or Activity Saturation Factor)

$\bar{\sigma}$ = average cross section, barns,

A_T = total dosimeter activity, M^{CI},

A_1 = dosimeter activity for cycle 1, M^{Ci},

t_1 = time from cycle 1 shutdown to cycle 3 shutdown,

N = Avogadro's number,

A_n = atomic weight of target material n,

f_i = fission yield of target isotope, 1.0 if not fissionable isotope,

F_j = fraction of full power during jth time interval, t_j,

λ_i = decay constant of the ith isotope,

T = sum of total irradiation time, i.e., residual time in reactor, and wait time between reactor shutdown and counting,

t_j = interval of power history,

τ_j = cumulative time from reactor start-up to end of jth time period, i.e.,

$$\tau_j = \sum_{k=1}^{j} t_k$$

Flux values at other locations are determined using ratios which account for well established azimuthal, axial and radial variations.

Reactor vessel fluence values are calculated as the sum of cycle 1 and cycles 2 plus 3 values: with the conservative assumption that the maximum value for all cycles fall at the same point on the reactor vessel ID.

The cycle 1 fluence values was obtained from the calculation for Capsule TE1-F.[1]

Vessel Fluence Extrapolation

For up-to-date operation, fluence values in the pressure vessel are calculated as described above. Extrapolation to future operation is required for prediction of vessel life based on minimum upper shelf energy (USE) and for calculation of pressure-temperature operation curves. Three time periods are considered: (1) to-date operation for which vessel fluence has been calculated, (2) designed future fuel cycles for which PDQ calculations have been performed for fuel management analysis of reload cores, and (3) future fuel cycles for which no analyses exist. Data from time period 1 are extrapolated through time period 2 based on the premise that excore flux is proportional to the fast flux that escapes the core boundary. Thus for the vessel,

$$\phi_{v,C} = \frac{\phi_{e,C}}{\phi_{e,R}} \times \phi_{v,R}$$

where the subscripts are defined as v = vessel, e = core escape, R = reference cycle, and C = a future fuel cycle. Core escape flux is available from PDQ output. Extrapolation from time period 2 through time period 3 is based on the last fuel cycle in 2 having the same relative power distribution as an "equilibrium" fuel cycle. Generally, the designed fuel cycles include several cycles into the future. Therefore, the last cycle in time period 2 should be representative of an "equilibrium" cycle. Data for TE1-B are listed in Table D-1.

This procedure is considered preferable to the alternative of assuming that lifetime fluence is based on a single, hypothetical "equilibrium" fuel cycle because this procedure accounts for all known power distributions. In addition, errors that may result from the selection of a hypothetical "equilibrium" cycle are reduced.

Table D-1. Extrapolation of Reactor Vessel Fluence

Cycle	Core escape flux, n/cm^2-s	Time, EFPY	Cumulative time, EFPY	Vessel flux, n/cm^2-s	Vessel fluence, n/cm^2	
					Time interval	Cumulative
1[a]	--	1.02	1.02	1.61(+10)	5.19(+17)	5.19(+17)
2&3[a]	0.648(+14)	1.56	2.58	2.01(+10)	9.88(+17)	1.51(+18)
4[b]	0.685(+14)	0.71	3.29	2.12(+10)[d]	4.8(+17)	2.0(+18)
5[b]	0.488(+14)	1.07	4.36	1.51(+10)[d]	5.1(+17)	2.5(+18)
X[c]	0.488(+14)	3.64	8	1.51(+10)[d]	1.7(+18)	4.2(+18)
X[c]	0.488(+14)	7	15	1.51(+10)[e]	3.3(+18)	7.6(+18)
X[c]	0.488(+14)	6	21	1.51(+10)[e]	2.9(+18)	1.0(+19)
X[c]	0.488(+14)	11	32	1.51(+10)[e]	5.25(+18)	1.6(+19)

[a] Calculated.

[b] Predicted.

[c] Extrapolated.

[d] Value from $\frac{0.685 \times 10^{14}}{0.648 \times 10^{14}} \times (2.01 \times 10^{10}) = 2.12 \times 10^{10}$.

[e] Cycle 5 assumed to be equilibrium cycle for future operation.

APPENDIX E

Capsule Dosimetry Data

Table E-1 lists the compostion of the threshold detectors and the equivalent cadmium thickness used to reduce competing thermal reactions. Table E-2 shows capsule TE1-F measured activity per gram of target material (i.e., per gram of uranium, nickel, etc.). Activation cross sections for the various materials were flux-weighted with a ^{235}U fission spectrum (Table E-3).

Table E-1. Detector Composition and Shielding

Monitors	Shielding	Reaction
10.4% U-Al (99.27% ^{238}U)	Cd-Ag 0.02676" Cd	$^{238}U(n,f)$
1.44% Np-Al (100% ^{237}Np)	Cd-Ag 0.02676" Cd	$^{237}Np(n,f)$
Ni 100% (67.77% ^{58}Ni)	Cd-Ag 0.02676" Cd	$^{58}Ni(n,p)^{58}Co$
0.66 wt % Co-Al (100% ^{59}Co)	Cd-0.040" Cd	$^{59}Co(n,\gamma)^{60}Co$
0.66 wt % Co-Al (100% ^{59} Co)	None	$^{59}Co(n,\gamma)^{60}Co$
Fe 100% (5.82% ^{58}Fe)	None	$^{54}Fe(n,p)^{54}Mn$

Table E-2. Dosimeter Specific Activities

Dosimeter material	Post irrad. wt, grams	Reaction	Radionuclide	Nuclide activity µCi	Specific activity µCi/g	Activity, µCi/g of target
Dosimeter: TE1 BD1						
Co-Al(Bare)	0.01578	$^{59}Co(n,\gamma)$	^{60}Co	37.26	2361	357800
Co-Al(Cd)	0.01748	$^{59}Co(n,\gamma)$	^{60}Co	8.508	436.8	66180
Ni	0.13543	$^{58}Ni(n,p)$	^{58}Co	188.5	1392	2054
Fe	0.15641	$^{54}Fe(n,p)$	^{54}Mn	10.64	68.03	1169
^{238}U-Al	0.08535	$^{238}U(n,f)$	^{137}Cs	0.06298	0.7379	7.095
^{237}Np-Al	0.06960	$^{237}Np(n,f)$	^{137}Cs	0.04056	0.5828	40.47
Dosimeter: TE1 BD2						
Co-Al(Bare)	0.01456	$^{59}Co(n,\gamma)$	^{60}Co	35.50	2301	348600
Co-Al(Cd)	0.01878	$^{59}Co(n,\gamma)$	^{60}Co	7.566	402.9	61040
Ni	0.13392	$^{58}Ni(n,p)$	^{58}Co	190.4	1422	2098
Fe	0.16241	$^{54}Fe(n,p)$	^{54}Mn	11.09	68.28	1173
^{238}U-Al	0.04593	$^{238}U(n,f)$	^{137}Cs	0.03515	0.7653	7.359
^{237}Np-Al	0.06833	$^{237}Np(n,f)$	^{137}Cs	0.03914	0.5728	39.78
Dosimeter: TE1 BD3						
Co-Al(Bare)	0.01487	$^{59}Co(n,\gamma)$	^{60}Co	21.88	1471	222900
Co-Al(Cd)	0.01968	$^{59}Co(n,\gamma)$	^{60}Co	5.390	273.9	41500
Ni	0.13768	$^{58}Ni(n,p)$	^{58}Co	137.5	998.7	1474
Fe	0.15176	$^{54}Fe(n,p)$	^{54}Mn	7.341	48.37	831.1
^{238}U-Al	0.05077	$^{238}U(n,f)$	^{137}Cs	0.02710	0.5338	5.132
^{237}Np-Al	0.06876	$^{237}Np(n,f)$	^{137}Cs	0.03209	0.4667	32.41

Table E-2. (Cont'd)

Dosimeter material	Post irrad. wt, grams	Reaction	Radionuclide	Nuclide activity μCi	Specific activity μCi/g	Activity, μCi/g of target
Dosimeter: TE1 BD4						
Co-Al(Bare)	0.01563	$^{59}Co(n,\gamma)$	^{60}Co	41.64	2664	403700
Co-Al(Cd)	0.01893	$^{59}Co(n,\gamma)$	^{60}Co	10.34	546.2	82760
Ni	0.13079	$^{58}Ni(n,p)$	^{58}Co	226.0	1728	2550
Fe	0.15279	$^{54}Fe(n,p)$	^{54}Mn	12.93	84.63	1454
^{238}U-Al	0.09187	$^{238}U(n,f)$	^{137}Cs	0.08709	0.9480	9.115
^{237}Np-Al	0.07075	$^{237}Np(n,f)$	^{137}Cs	0.05345	0.7555	52.46

Footnotes - Dosimeter Material Data

These data are the disintegration rates per gram of wire, as of 1200 hours, July 25, 1983.

These data are the disintegration rates per gram of target nuclide: viz., ^{238}U, ^{237}Np, ^{58}Ni, ^{59}Co, and ^{54}Fe.

The following abundances and weight percents were used to calculate the disintegration rate per gram of target element.

^{238}U - 10.4 wt %; 99.27% target nuclide.

^{237}Np - 1.44 wt %; 100% target nuclide.

Ni - 100 wt %; 67.77% ^{58}Ni target nuclide.

Co - 0.66 wt %; 100% ^{59}Co target nuclide.

Fe - 100 wt %; 5.82% ^{54}Fe target nuclide.

Table E-3. Dosimeter Activation Cross Sections, b/atom[a]

G	Energy range, MeV	$^{237}Np(n,f)$	$^{238}U(n,f)$	$^{58}Ni(n,p)$	$^{54}Fe(n,p)$
1	12.2 - 15	2.323	1.050	4.830(-1)	4.133(-1)
2	10.0 - 12.2	2.341	9.851(-1)	5.735(-1)	4.728(-1)
3	8.18 - 10.0	2.309	9.935(-1)	5.981(-1)	4.772(-1)
4	6.36 - 8.18	2.093	9.110(-1)	5.921(-1)	4.714(-1)
5	4.96 - 6.36	1.541	5.777(-1)	5.223(-1)	4.321(-1)
6	4.06 - 4.96	1.532	5.454(-1)	4.146(-1)	3.275(-1)
7	3.01 - 4.06	1.614	5.340(-1)	2.701(-1)	2.193(-1)
8	2.46 - 3.01	1.689	5.272(-1)	1.445(-1)	1.080(-1)
9	2.35 - 2.46	1.695	5.298(-1)	9.154(-2)	5.613(-2)
10	1.83 - 2.35	1.677	5.313(-1)	4.856(-2)	2.940(-2)
11	1.11 - 1.83	1.596	2.608(-1)	1.180(-2)	2.948(-3)
12	0.55 - 1.11	1.241	9.845(-3)	6.770(-4)	6.999(-5)
13	0.111 - 0.55	2.34(-1)	2.432(-4)	1.174(-6)	1.578(-8)
14	0.0033-0.111	6.928(-3)	3.616(-5)	1.023(-7)	1.389(-9)

[a] ENDF/B5 values have been flux-weighted (over CASK energy groups) based on a ^{235}U fission spectrum in the fast energy range plus a 1/E shape in the intermediate energy range.

APPENDIX F

References

1 A. L. Lowe, Jr., et al., Analysis of Capsule TE1-F Toledo Edison Company, Davis-Besse Nuclear Power Station Unit 1, BAW-1701, Babcock & Wilcox, Lynchburg, Virginia, January 1982.

2 H. S. Palme, G. S. Carter, and C. L. Whitmarsh, Reactor Vessel Material Surveillance Program -- Compliance With 10 CFR 50 Appendix H, for Oconee-Class Reactors, BAW-10100A, Babcock & Wilcox, Lynchburg, Virginia, February 1975.

3 A. L. Lowe, Jr., K. E. Moore, and J. D. Aadland, Integrated Reactor Vessel Material Surveillance Program, BAW-1543, Rev 1, Babcock & Wilcox, Lynchburg, Virginia, October 1983.

4 A. L. Lowe, Jr., et al., Fracture Toughness Test Results From Capsule TE1-B, The Toledo Edison Company, Davis-Besse Nuclear Power Station Unit 1, BAW-1835, Babcock & Wilcox, Lynchburg, Virginia (to be published).

5 J. D. Aadland, R. J. Futato, and W. A. Pavinich, Babcock & Wilcox J-R Test Procedure for Compact Fracture Toughness Specimens, BAW-1808, Babcock & Wilcox, Lynchburg, Virginia, October 1983.

6 H. S. Palme and H. W. Behnke, Methods of Compliance With Fracture Toughness and Operational Requirements of Appendix G to 10 CFR 50, BAW-10046A, Rev 1 Babcock & Wilcox, Lynchburg, Virginia, July, 1977.

7 A. L. Lowe, Jr., et at., Irradiation-Induced Reduction in Charpy Upper Shelf Energy of Reactor Vessel Welds, BAW-1511P, Babcock & Wilcox, Lynchburg, Virginia, October 1980.